JPhys Materials

PAPER • OPEN ACCESS

Interaction of xanthan gums with galacto- and glucomannans. Part II: Heat induced synergistic gelation mechanism and their interaction with salt

Journal of Physics: Materials

PAPER

Interaction of xanthan gums with galacto- and glucomannans. Part II: Heat induced synergistic gelation mechanism and their interaction with salt

Marta Ghebremedhin[1], Christine Schreiber[1], Birgitta Zielbauer[1], Natalie Dietz[2] and Thomas A Vilgis[1]

[1] Max-Planck-Institut für Polymerforschung, Department of Polymer Theory, Food science and statistical physics of soft matter, Ackermannweg 10, 55128, Mainz, Germany
[2] Jungbunzlauer Ladenburg GmbH, Jungbunzlauer Suisse AG, Dr. Albert-Reimann-Straße 18 68526, Ladenburg, Germany

E-mail: ghebre@mpip-mainz.mpg.de **and** vilgis@mpip-mainz.mpg.de

Keywords: xanthan gum, guar gum, locust bean gum, konjac glucomannan, heat induced gelation mechanism, molecular interactions, synergism,

OPEN ACCESS

RECEIVED
21 April 2020

REVISED
26 May 2020

ACCEPTED FOR PUBLICATION
9 June 2020

PUBLISHED
7 July 2020

Abstract

In this study the heat induced synergistic gelation of different hydrocolloid solutions, xanthan gum types (XG) in mixture with galactomannans like guar gum (GG), locust bean gum (LBG) and konjac glucomannan (KGM) is investigated. The physical mechanism of the synergy in thickening and gelling of blends depends on the monomer structure, the molecular weight, the charge, the polarity, and the chain stiffness of the hydrocolloids. Particularly the properties of the electrically neutral galacto- and glucomannans mixed in combination with xanthan gum strongly affect the synergistic effects. These are influenced by the number and distribution of mannan side chains and thus their flexibility. While the pure components do not show gelation on their own, they form viscoelastic solutions or even gels when mixed together and heated. In this study, rheological properties of the resulting composite gels of 0.5% (w/w) were examined under different physicochemical and thermal conditions. Focus was laid on thermally induced gels, as these gels showed higher synergistic effects compared to the non-heated ones. The gelation mechanisms were investigated by strain and temperature dependent oscillatory rheological measurements. Blends with XG-GG (20:80) showed the weakest synergism, followed by XG-LBG blends (20:80), whereas XG-KGM (60:40) blends showed the highest increase of the storage modulus. This can be explained by different local interactions in combinations with the flexibility of the various components. Furthermore, the impact of monovalent salt on the interactions was investigated. Addition of sodium chloride at 0.05% and 0.5% (w/w) concentrations influenced the gelling due to Coulomb screening of the negative charges of XG. Consequently, the synergism, in particular the storage modulus, is strongly affected by variation in salt concentration. We propose specific models based on the gel formation in case of XG-LBG and XG-KGM blends, whereas XG-GG shows an entropic phase separation due to flexibility of GG.

1. Introduction

Hydrocolloids are widely used in the food, cosmetic and pharmaceutical industry due to their vast range of functional properties. To improve quality and texture, they are mainly used as emulsifiers, stabilizers, thickeners and gelling agents and find versatile uses in sauces, soups, jams, fruits, jellies and beverages but also in body and dental care products [1]. Hydrocolloids can be polymers like polysaccharides, which have a thickening and gelling effect when hydrated in water above a critical concentration.

In the present paper, non-gelling thickeners such as xanthan gum, galacto and glucomannan are investigated. Their combinations are known to form gels and thus are often used to exploit their synergistic effects in order to optimize and generate novel textural properties. The interest in the use of polysaccharide

blends in food is due to their ability to modify and improve the rheological properties i.e. to precisely control the texture and viscoelastic properties and provide a better mouth feeling.

The rheological properties of hydrocolloids depend on their chemical structure as well as on intra- and intermolecular interactions by hydrogen bonding, electrostatic interaction, hydrophobic interaction and steric exclusion. These interactions can be influenced by the solvent as well as conditions such as temperature, ionic strength, shear and pH [2]. However, the extent of viscosity change varies depending on the type of hydrocolloids and is based on interaction between nonspecific and disordered entanglements of the polymer chains. This interaction increases with the concentrations, where the critical concentration c^* is the overlap concentration [1, 3, 4]. In addition, the viscosity is also influenced by the chain stiffness and the electrostatic charge density.

While most hydrocolloids produce thick and viscous solutions, very few have the ability to form gels. As the gels also differ significantly in moduli, fracture properties and thus texture, knowledge and understanding of the gelation mechanism is necessary for the design of food formulations. The property of gelation is based on the association of polymer chains whose compounds show an ordered conformation of a three-dimensional network in which the water is immobilized. Hydrocolloid gels are formed by cross-linked polymer chains, held together by physical intermolecular interactions, like hydrogen bonding, hydrophobic and ionic interaction. In addition, according to de Gennes *et al* [5] there is a direct correlation between the mesh size ξ and the modulus of elasticity or gel strength for permanently cross-linked gels [5, 6].

The primary structure of the bacterial polysaccharide xanthan, which is produced by *Xanthomonas campestris,* is given by a β-(1→4)-D-glucose cellulose backbone of high molecular weight. At every second glucose residue there is a linked α-(3→1) negative charged trisaccharide side chain. This side chain consists of two mannose units and a glucoronic acid in between. The internal mannose of the side chain contains an acetyl group at the C-6 position, while the terminal mannose contains a pyruvate residue linked between the C-4 and C-6 position [7–9]. Xanthan molecules are highly charged and are considered as rigid rod-like polymers, which is why its thickening effect is explained by a jamming transition. The jamming transition is caused by immobilization of the rigid xanthan molecules at random positions and orientations due to electrostatic repulsion of the negatively charged side chains according to the Coulomb interaction [10, 11]. Furthermore, x-ray structure analysis revealed the secondary structure of xanthan gum. They showed a right-handed five-fold helix conformation. Electrostatic repulsion of the negative side chains stabilizes the helix structure and leads to this rigid, ordered structure [12]. In deionized water and at concentration up to about 0.3% xanthan gum undergoes a conformational change upon heating at around 40 °C or by addition of ions [9, 13]. There is a transition from a stiff, rigid and ordered helix structure at low temperature and low ionic concentration to a disordered, flexible structure at high temperature and high ionic concentration. The presence of the functional groups of the side chains influences this transition [13].

The galactomannans locust bean gum (LBG) and guar gum (GG) that are extracted from plants seeds consist of a linear chain of β-(1→4)-D-mannopyranose backbone with side chains of (1→6)-linked α-D-galactosepyranosyl unit [14, 15]. They can be characterized by their content of galactose side chains, i.e. by molar ratio of D-mannose to D-galactose. The mannose:galctose ratio is approximately 4:1 for LBG and 2:1 for GG [16–18].

The chemical structure of konjac glucomannan (KGM), extracted from plants is composed of a linear backbone of (1→4)-linked β-D-glucopyranose and β-D-mannopyranose in random order. As side chains, acetyl groups randomly occur on the C2, C3 or C6 to the mannopyranose units [19]. Studies with x-ray diffraction, CD spectroscopy and UV–Vis spectroscopy have been carried out to demonstrate that konjac forms two-fold single helices in solution stabilized by intramolecular O-3—O-5' hydrogen bonds. This single-helix conformation seems to be a crucial and important factor for the resulting physicochemical properties [20, 21]. Furthermore, it was observed that KGM undergoes a temperature-induced conformational change from the ordered helix structure at low temperature into a flexible disordered structure at higher temperature. This transition occurs at $\geqslant$60 °C [21].

The synergistic effects and the precise gelation mechanisms of xanthan and galacto- and glucomannan are still being discussed. One of the earliest studies proposed a molecular interaction between the unsubstituted mannan backbone and the xanthan in its ordered helix conformation [22]. Later studies, however, assumed an interaction between the unsubstituted mannan backbone and the backbone of the disordered xanthan molecule [23]. In the literature, rheological investigations on synergistic gelation or thickening and thus on molecular interaction between xanthan and galacto- and glucomannan have been conducted in numerous studies over the last decades. Rheology has become a well established technique to gain insights into the relationship between the cooperative associations of polymer chains i.e. their cross-links, leading to network formation and rheological properties, such as gel strength. Different methods such as oscillatory-shear measurement, were used to characterize the interplay of different modified xanthan types and galacto- and glucomannan, forming a strong thermo-reversible gel network and synergistic

gelation. Temperature and strain dependent measurements were performed on the mixed systems. Such studies showed a correlation between the cooperative association of the polymer chains and the viscoelastic moduli [24–26]. Other researchers examined dynamic viscoelasticity of xanthan and galacto- and glucomann mixtures and proposed an intermolecular interaction between the xanthan side chain and the backbone of the galacto- and glucomannan by hydrogen bonding [27–29]. There a many proposed theories of different gelation mechanisms. Further investigations indicate different interaction and gelation mechanisms, characterized by temperature dependent rheological measurements. It was found that the gel formation undergo several process steps dependent on polysaccharide conformation and temperature transition as well as conditions such as ionic strength [30]. Moreover, the impact of the resulting composite gels on the viscoelastic properties was shown [31].

The effects of the synergisms depend strongly on the different molecular structure of the galacto- and glucomannans, especially influenced by the number and distribution of the side chains. The chemical structure of xanthan also plays a role in the impact of the synergy effects. These findings were supported by x-ray studies on synergistic interaction [23, 32, 33]. Previous optical-rotational studies have confirmed that intermolecular interactions occur between the helical backbone of the xanthan gum and the backbone of the unsubstituted regions of the galacto and glucomannans, leading to cross-linkages due to their association [11, 23, 34, 35].

The observation that the synergistic effect depends on the mannose-galactose ratio of the galactomannan, i.e. the ratio of the numbers of respective side chains, was consistent in all studies. Guar gum has the most side chains with a ratio of 2:1, which led to the assumption the intermolecular interaction between the mannan backbone and the xanthan gum is impeded by steric hindrance [15]. Locust bean gum has fewer side chains with a mannose-galactose ratio of 4:1 [14]. From this, it was concluded that due to the large galactose-free regions, increased intermolecular bonding between the mannan backbone and the xanthan gum may take place [36]. It is also supposed that konjac glucomannan has better intermolecular interactions with xanthan due to its very few side chains [37].

Despite this relatively high number of studies, the precise gelation mechanism for all different systems from a physicochemical point of view is still not yet fully understood [11, 23, 28, 29, 38]. Investigations of the non-heated mixed systems showed strengthening effects, which are, however, much less pronounced than the heated mixtures. This leads to the assumption that when the polysaccharides are heated, temperature-induced conformational changes as well as physicochemical effects occur which cause this strengthening of the gelation.

In the first part of this project, the molecular interactions of the same mixed system as studied here were investigated without heat-induced cross-linking. Thereby the single components and the mixtures were characterized by rheology and atomic force microscopy. By using AFM images of guar gum, locust bean gum and konjac glucomannan, the shapes of these molecules were characterized and the persistence lengths of the different xanthan types were determined to compare chain stiffness.

In this part of the study, the focus was drawn on the investigation of the thermally induced gelation. In order to understand why this heating step is required to achieve the significantly higher synergistic effects compared to the non-heated mixture. Rheological characterization, namely amplitude and temperature sweeps, was used to analyse the synergistic effects. Furthermore, the impact of salt on the interaction was investigated. In addition, we propose specific models based on these results to describe the gelation mechanism between xanthan and mannan.

2. Materials and methods

2.1. Materials

The four different types of xanthan gum used in this study were obtained from Jungbunzlauer Ladenburg GmbH in Germany. Xanthan gum 1 (XG1) is an unmodified xanthan ($M_w = 1{,}35{*}10^6$ g mol^{-1}), xanthan gum 2 (XG2) contains less pyruvate groups and has the least molecular weight ($M_w = 1{,}08{*}10^6$ g mol^{-1}), xanthan gum 3 (XG3) contains hardly any acetate groups and has the highest molecular weight ($M_w = 1{,}68{*}10^6$ g mol^{-1}), and xanthan gum 4 (XG4) includes calcium ions, since the pH value during fermentation is adjusted using $Ca(OH)_2$ [39]. Locust bean gum (VIDOGUM L 175), guar gum (VIDOGUM G200 I), and konjac glucomannan (VIDOGUM KJ-II) were obtained from UNIPEKTIN AG, Eschenz, Switzerland.

2.2. Sample preparation

All hydrocolloids were dissolved in Milli-Q water, to obtain an absolute concentration of 0.5% w/w and taking into account the moisture content of the hydrocolloids by the following equation:

$$m_x = \frac{0.5\,\% * 10\,g}{100\,\% - MC\%}$$

(m_x: mass of xanthan, MC: moisture content).

The moisture content of the samples was determined by a halogen moisture analyzer (Mettler Toledo HR83) by using 10 g of a solution with 0.5% w/w hydrocolloid.

The required amount of hydrocolloid was slowly added to the corresponding amount of water with stirring on a magnetic stirrer (xanthan: 350 rpm, gluco-galactomannan: 500 rpm). As locust bean gum (LBG) is partly soluble at room temperature and fully soluble in hot water, LBG was additionally heated for 10 min at 90 °C–95 °C with stirring. To ensure complete solubility, all samples were stirred overnight at room temperature. To remove cell residues, the dispersions of locust bean gum, guar gum and konjac glucomannan were centrifuged at 1035 rpm (15 090 g) and the supernatant was carefully decanted. The xanhan and mannan mixtures were prepared with pure dissolved samples in various ratios in 20 ml snap-cap bottles and heated to 85 °C with stirring (1200 rpm). To avoid any evaporation while measuring the temperature, the contact thermometer was inserted through the plastic lid of the snap-cap bottle.

For the amplitude sweep measurements, disposable plates made of aluminum with a 25 mm diameter and a height of 3 mm were used. Teflon molds were used with an inner diameter of 25 mm and a height of 6 mm, which were slipped over the aluminum plates. To produce the gels the still hot mixture of hydrocolloid was pipetted onto the Teflon mold and evenly distributed with a razor blade to obtain gels with a defined thickness of 3 mm. Then the mixtures of hydrocolloids were cooled down to room temperature and hardened in the refrigerator at 4 °C overnight. In order to reduce evaporation of water, the gels were covered with disposable weighing dishes greased at the edges to make them as airtight as possible. The following day, the molds were gently removed, and ensured the samples adapted to room temperature before measurements.

For the temperature sweep, the hydrocolloid mixtures were prepared as described above and heated up to 85 °C with stirring (1200 rpm). The hot mixture was pipetted onto the plate of the rheometer before measurement. Figure 1 shows a schematic overview of the sample preparation.

Sample preparation of the hydrocolloids dispersion with salt was conducted in the same manner as described above, by adding sodium chloride to the solved hydrocolloid to obtain 0.5% w/w and 0.05% w/w NaCl hydrocolloid dispersion.

2.3. Rheological measurements

Dynamic viscoelastic measurements of all hydrogel samples were performed in triplicate on a Discovery HR-3 Rheometer (TA Instruments), by amplitude and temperature-dependent oscillatory measurements using parallel plates with different diameter.

The amplitude sweep was conducted to examine the viscoelastic properties of the xanthan-mannan mixture gels. This method was used to measure storage (G') and loss (G'') moduli, to describe the deformation behaviour of the resulting composite gels in the non-destructive range namely linear viscoelastic (LVE) range as well as to determine the upper limit of this range. In addition, the characterization of the behaviour after exceeding this range is also of interest as the deformation increases until the inner structure of the gelled sample ruptures. In the present study, a viscoelastic character of the mixtures with values of $G' > G''$ in the LVE range is expected, indicating a predominantly elastic behaviour or solid-like structure due to network formation. The oscillation deformation was applied at constant frequency $f = 1$ Hz and the storage G' and loss G'' moduli were analysed as a function of the strain γ in the range between 0.01% and 1000 %. The measurements were carried out with a 25 mm diameter plate at a constant temperature of 25 °C with a soaking time of 120 s. Because the height of the different gels deviated from the intended 3 mm, the gap size between the two plates had to be varied and set between 2500 μm and 2900 μm before measuring, in order to ensure sufficient adhesion to prevent the upper plate from slipping off the sample as well as slippage or rupture of the sample during measurement. Therefore, an appropriate pressure had to be applied on the sample between the plates. However, it should also be avoided pressing the plate too hard on the sample, since this could lead to a small deformation or even destruction of the sample. Based on preliminary measurements, an axial force of 0.05 N for the more elastic mixture and 0.02 N for more viscous mixtures, was applied in order to get appropriate contact for the amplitude test.

The temperature sweep provides information about the temperature-dependent viscoelastic behavior of the different xanthan-mannan compositions and their gelation mechanisms. This method allows the investigation of the sol-gel transition and thus the determination of the gelation point T_{gel}, which is the crossover point $G' = G''$. As the mixtures presented in this study exhibited a predominantly elastic behaviour at room temperature, a sol-gel transition is expected in all mixtures.

Since the crossover points of the storage and loss moduli ($G' = G''$) varied greatly during the cooling process of the XG-GG blends, T_{gel} was determined as the temperature at the inflection point of the G' curve, having the highest change in the G'-value, to ensure the reproducibility of the gel point determination.

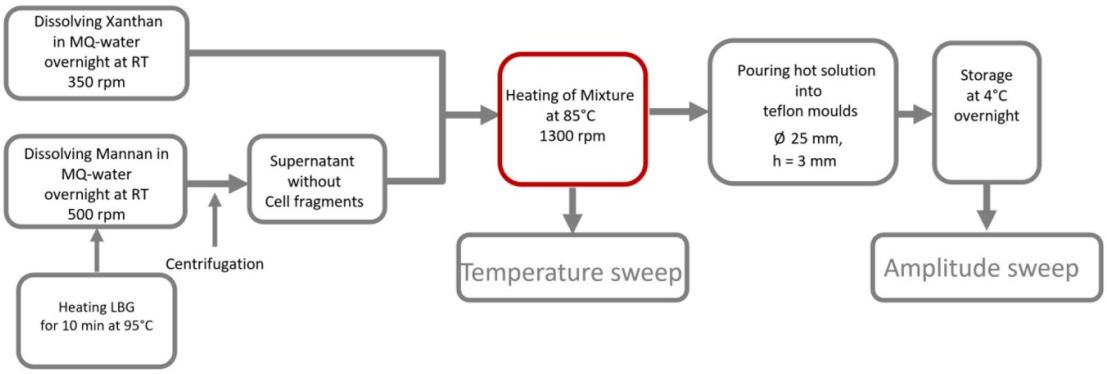

Figure 1. Schematic of the sample preparation.

Therefore, samples were prepared as usual but instead of cooling them to form gels, they were transferred via pipette in their heated sol-state on the 85 °C pre-heated peltier plate. Storage G' and loss G'' moduli were measured depending on the temperature at constant frequency $f = 1$ Hz and strain $\gamma = 0.01$ %. The measurements were performed in a triplet determination using a 40 mm diameter plate and a solvent trap to prevent evaporation. The pre-set distance between the plates was 500 μm, which corresponds to a sample volume of approx. 650 μl. Furthermore, a soak time of 300 s was observed in order to ensure an equilibrium of the systems in the measuring sample before starting the measurement. The liquid samples were cooled down from 85 °C to 10 °C and reheated to 85 °C at a rate of 1 °C min^{-1}.

2.4. Zeta potential

Zetapotential measurements were carried out on a Zetasizer Nano ZS (Malvern Germany) for XG1 and XG2 (0.001% w/w) at different sodium chloride concentrations (0 mM, 0.1 mM, 0.5 mM, 1 mM, 5 mM, 10 mM, 50 mM, 100 mM, 500 mM) at 25 °C. This was used to determine the NaCl concentrations for subsequent temperature-dependent oscillation measurements. To prevent multiple scattering effects, zeta potential measurements were performed at a much lower concentration of sample, than the ones used in the rheological measurements. The ξ-potential provides information about the effective charge of particles in solution and their electrophoretic mobility when an electrical field is applied. The velocity of the particles is measured using a laser light scattering method based on a laser Doppler anemometry and was calculated using the Helmholtz-Smoluchowski equation.

3. Results and discussion

To investigate the synergism of the XG-GG, XG-LBG and XG-KGM blends, xanthan samples differing in molecular weight, functional group, charge and flexibility were used and compared by various rheological measurements. By using amplitude sweeps, the elastic and viscous moduli (viscoelastic properties) of the gelled systems were investigated to determine the different synergism effects and thus conclusions were drawn about the interactions of the mixtures. Subsequently, the gelation process was investigated using temperature-dependent oscillation measurements in order to compare and understand the gelation mechanism between the different types of xanthan gum and mannan in the mixtures. Furthermore, the impact of salt on the gel properties and the gelation process were investigated by carrying out a temperature sweep.

3.1. Viscoelastic properties

In order to understand the systems of the pure components, the results of the amplitude sweeps of the individual components are shown in figure 2.

Figure 2(a) shows the mean values and their standard deviations of the elastic and viscous moduli as a function of the strain for the individual xanthan types. For all xanthan types, G' and G'' exhibit a constant linear behavior with a constant value of G' and G'' followed by a decrease as the applied strain becomes very high. Furthermore, the unmodified XG1, the XG4 which contains calcium ions as well as the deacetylated XG3 show the same storage modulus G' at about 5 Pa. Loss moduli G'' of all three samples show the same value at about 2 Pa. In the case of these three types of xanthan gum, the storage moduli are higher than the respective loss moduli, i.e. they exhibit properties of a gel. The G' moduli of the pyruvate-poor xanthan XG2 are about 3 Pa lower than those of the other xanthan types. XG2, which reveals a G' just below the G'', has the

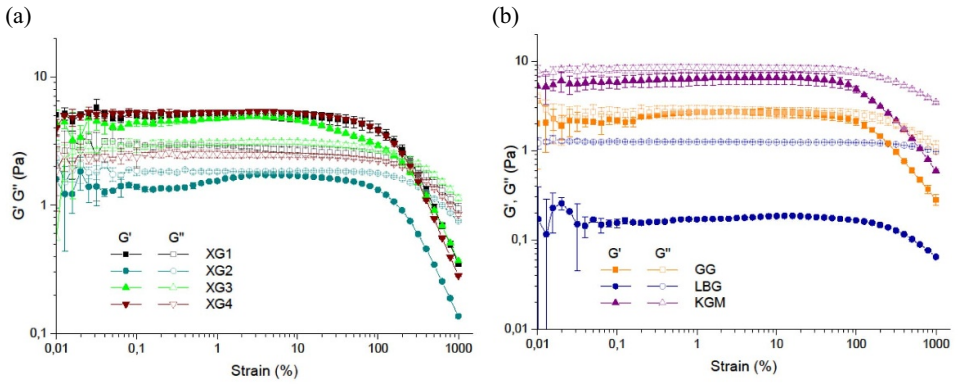

Figure 2. Result of mean values of the amplitude sweep measurements of the (a) 0.5% w/w xanthan gum types (XG) and of (b) 0.5% w/w guar gum (GG), locust bean gum (LBG) and konjac glucomannan (KGM). Dependence of G′ (filled symbols) and G″ (empty symbols) on strain at constant frequency ($f = 1$ Hz) and temperature (T = 25 °C).

weakest gel character. Figure 2(b) displays the mean values of G' and G'' with their standard deviations for guar gum, locust bean gum and konjac glucomannan. The mannans show a different behavior than the xanthan gums, all of them exhibit a higher value for G'' than for G'. Thus, their viscous behavior dominates over the elastic one. The storage and the loss moduli of the mannan samples differ more distinctly from each other. KGM shows with approx. 5 Pa the highest storage modulus, whereas the storage modulus of the GG is slightly lower with a value of 2 Pa. For both KGM and GG, the loss moduli are slightly above the storage moduli. On the contrary, LBG has the lowest value for the storage modulus with 0.2 Pa and shows the largest difference in value between the loss and the storage moduli. This indicates a stronger viscosity dominated behavior of LBG compared to GG and KGM and thus LBG does not form a gel.

To determine the mixing ratio of the xanthan-mannan blends with the highest synergism, amplitude-dependent measurements were performed to obtain information about their storage and loss moduli. In addition, it was investigated how the viscoelastic properties change depending on the blend ratio.

For comparison of the different xanthan-mannan blends synergisms, figure 3 shows mean values of the storage and the loss moduli G', G'' depending on the xanthan concentration at a constant strain of $\gamma = 1$ %. To determine the strength of synergism, only the storage modulus G' was considered. Since the different xanthan gum types exhibit similar synergisms in the mixing ratios with the respective mannans, only mixtures of XG with GG, LBG and KGM will be discussed as examples for the xanthan-mannan blends in the following.

When comparing the mixtures with the individual components, the xanthan blends with guar gum show a slight increase in the elastic modulus. Furthermore, the values of the storage moduli of the XG-GG systems with different mixing ratios hardly differ from each other. On the other hand, the storage modulus of the mixtures with LBG increases considerably compared to the individual components. While the XG-GG blends show a G' increase of less than 20 Pa and the weakest synergism effect, the XG-LBG blends for a ratio of 20:80 show with a maximum of approx. 100 Pa a stronger synergism. The KGM blends exhibit the highest increase of the storage modulus G' and for the ratio of 60:40 for XG-KGM a maximum value of about 400 Pa is found and thus reveal the highest synergism.

In order to investigate how the synergy effects of the individual xanthan gum types differ in the mixed systems, amplitude tests were performed for the ratios possessing the highest storage modulus G'. As previously determined, this corresponded to a ratio of 60:40 for XG-KGM and 20:80 for XG-LBG and XG-GG, respectively.

Figure 4 shows the results of the amplitude sweeps of the respective galacto and glucomannan blends with the different xanthan types. In figure 4(a) all XG-GG show similar trends with a linear viscoelastic (LVE) range followed by a decrease. The guar gum mixture with XG3, which has a very low number of acetate groups, displays the highest storage modulus G', followed by the mixtures with unmodified XG1, and XG4 which contains calcium ions. The lowest synergism is found in the guar mixtures with the pyruvate-poor XG2.

Regarding the xanthan blends with locust bean gum (see figure 4(b)), the mixture with XG3 shows the highest increase in the storage modulus G'. All mixtures show a G' maximum with increasing deformation when exceeding the LVE range prior to a final decrease. This could be a sign of strain hardening. Due to

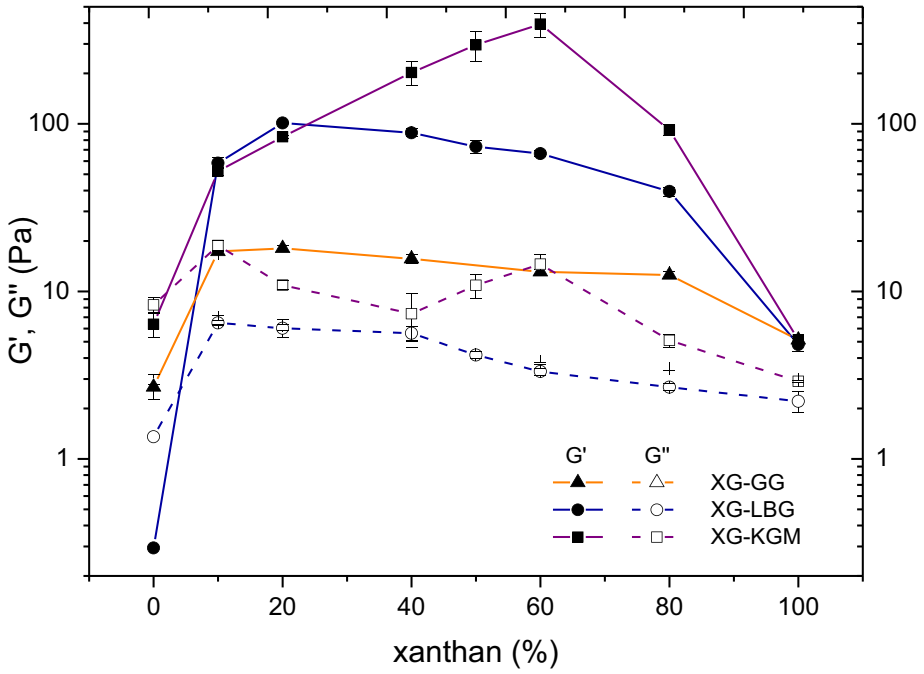

Figure 3. Mean values of storage (G') and loss (G'') moduli of 0.5% w/w xanthan blends with guar gum (GG), locust bean gum (LBG) and konjac glucomannan (KGM) plotted logarithmically depending on the xanthan concentration at a constant strain of $\gamma = 1$ %.

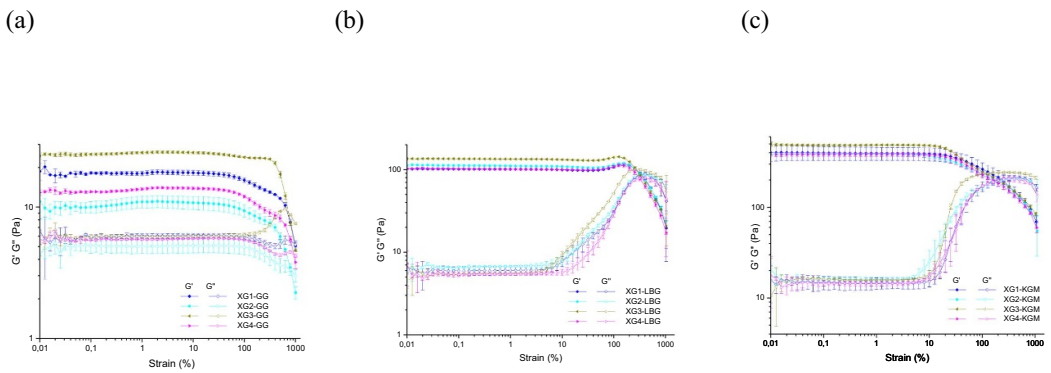

Figure 4. Mean values of G' and G'' of the amplitude sweep measurements of 0.5% w/w (a) xanthan blends with guar gum in a ratio of 20:80, (b) xanthan blends with locust bean gum in a ratio of 20:80 and (c) xanthan blends with konjac in a ratio of 60:40. Storage and loss moduli G' (filled symbols), G'' (empty symbols) are plotted in logarithmic terms with respect to the strain at a constant frequency ($f = 1$ Hz) and temperature ($T = 25$ °C).

cross-linking, greater force is required with increasing deformation, since the polymer chains are stretched by pulling them apart and the network becomes firmer. All XG-LBG blends also exhibit a significant increase and a maximum of the loss modulus G'' prior to a final decrease. This trend of the G'' peak with increasing deformation points to a gel network structure due to cross-linked polymers in these blends. The rise of G'' is an indication of an increase in the deformation energy, which is transferred to the environment before the final rupture of the inner structure of the entire sample, and parts of the inner structure are irreversibly deformed. Thus, deformation energy is lost and converted into frictional heat. The occurrence of the G'' hump could be explained by relative movement of molecules, free chain ends, flexible side chains or long network bridges that are not permanently embedded in the network [40].

For the blends with konjac in figure 4(c) the same trend of G' increase can be observed with respect to the different xanthan types. Again, it can be seen that the graphs of the different xanthan gums for the respective galacto- and glucomannan hardly differ. In comparison to the LBG blends, the KGM blends also show an increase in the loss modulus G'' at large deformation (strain). However, the LVE range of the storage modulus is shorter and no hump is depicted. This indicates that the konjac blends are more rigid than the

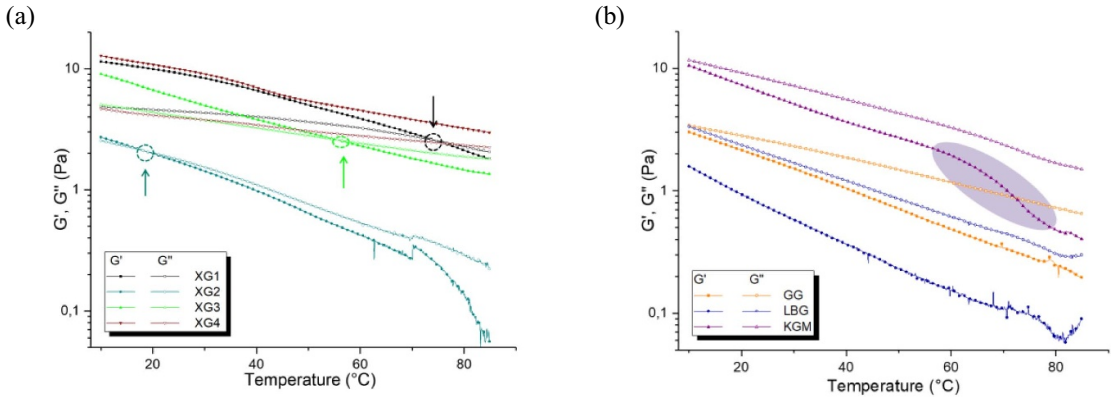

Figure 5. Results of temperature sweep (a) of 0.5% w/w xanthan types and (b) 0.5% w/w galacto- and glucomannan. Logarithmic plot of the average storage and loss moduli G′ (filled symbols), G″ (empty symbols) versus temperature at constant frequency ($f = 1$ Hz) and strain ($\gamma = 1$ %).

LBG blends and therefore more easily destroyed by deformation. The LBG blends are more flexible and can resist higher deformations until the network is finally destroyed.

In both systems of LBG and KGM blends, micro cracks could occur in the network indicated by the rise of G'' after exceeding the limit of the LVE range. Furthermore, it is assumed that at the maximum of G'' these grow into macro cracks until finally the entire network is destroyed.

3.2. Temperature-dependent behaviour

Temperature-dependent oscillation measurements were performed to investigate the gelation process by observing the dependence of the viscoelastic behavior on temperature, hence the 'sol-gel' transition.

3.2.1. Xanthan types

Figure 5(a) shows the viscoelastic behavior of the four different xanthan types dependent on temperature.

As expected, for all tested types of xanthan there is an increase in moduli with decreasing temperature. This is because the movement of the xanthan molecules decreases as the temperature is reduced. When the molecular dynamics slow down during cooling, they begin to immobilize and 'freeze' by random blocking due to the repulsion of negative charges. If the stiffened molecules now experience an external force but block each other, this so-called 'jamming effect' leads to an increase in moduli [41]. Even if the xanthan molecules are more mobile at high temperatures, their dynamic is still limited due to the negative charges on their side chains. Because of these numerous negative charges, it is likely that xanthan molecules are still stiff at high temperatures even if they are not in the helical configuration. This leads to the conclusion, that the coil-helix transition hardly influences the viscosity change of the xanthan gum.

With exception of XG4, which contains calcium ions, all other xanthan gums show a crossing point between G' and G''. In addition, XG4 shows the smallest change in storage and loss moduli values with temperature change, displays nearly parallel curves, and thus shows a G' dominated behavior over the whole temperature range. These observations for XG4 indicate that it has the highest thermal stability among the tested xanthan samples. Bonds between the negatively charged xanthan molecules and the presence of Ca^{2+} counter ions could explain the fact that XG4 has a pronounced gel character even at high temperatures, since a strong cross-linking leads to stiffer and larger molecule assemblies. The remaining xanthan types show a sol-gel transition during cooling where the storage and loss moduli intersect. The pyruvate-poor XG2 shows the lowest moduli and a sol-gel transition at low temperature about 18.1 °C. The moduli of the deacetylated XG3 exhibit higher values than those of XG2 and the sol-gel transition occurs at about 55.5 °C. The unmodified XG1, which has the second highest G' value, shows a crossing of G' and G'' at the highest temperature about 74.6 °C. Furthermore, XG2 shows the greatest temperature dependency of G' and G'' and has the lowest moduli compared to all the other types of xanthan gum. According to the work of Wehr *et al* [39], XG2 contains less pyruvate groups and thus the least number of negative charges. Additionally, it has the lowest molecular weight. This leads to the conclusion that during cooling, the molecules of XG2 are less immobilized and their 'jamming' is less likely. Due to the fewer number of negative charges, the mutual repulsion of the xanthan gum molecules decreases. At the same time the critical concentration, and thus the occurrence of the 'jamming effect', depends on the molecular weight, the length and charge of the molecules [41]. In addition, the negative side chains in the helix conformation of the xanthan try to avoid each other due to repulsion. Finally, the fewer number of negative side chains in XG2 can result in having to apply less

Table 1. Average of the gelation temperature T_{gel} and storage moduli G' at 25 °C for the XG-GG blends.

Mixtures	T_{gel} (°C)	SD	G' (Pa) (25 °C)	SD
XG1-GG	22.54	±0.51	12.06	±2.41
XG2-GG	22.53	±0.49	7.03	±1.84
XG3-GG	26.93	±0.29	17.97	±1.54
XG4-GG	21.53	±0.51	8.33	±0.82

thermal energy to overcome these electrostatic repulsions. The helix structure of XG3 is less stable due to the fewer number of acetyl residues. Since it also has more hydroxyl groups, which can form hydrogen bonds with the surrounding water, XG3 is more soluble in water compared to XG1. As a result, the disordered, rather hydrophobic polymer chains of XG1 interact via non-specific entanglements, resulting in increased moduli. Finally, a relationship between the G' values and the crossing point of G' and G'' can be seen. XG4, which has no crossing point, displays the highest storage modulus G'. The remaining xanthan types point out that the lower the G', the lower the temperature at which $G' = G''$ is found.

3.2.2. Galacto- and glucomannan

Figure 5(b) shows the dependency of the storage (G') and loss (G'') moduli on temperature of guar gum, locust bean gum and konjac glucomannan solutions. As with xanthan, an increase in moduli with decreasing temperature can be observed. However, for all mannans a dominant viscous behavior can be detected throughout the entire temperature range: even at low temperatures, values of $G'' > G'$ were found. As found earlier, konjac shows the highest G', followed by guar gum, which has a higher G' than locust bean gum due to its higher molecular weight. The temperature-dependent behavior of guar gum and locust bean gum is a result of a temperature effect and thus viscosity change according to Arrhenius instead of a structural change. Konjac shows a conspicuously high change of moduli at approx. 60 °C. This could be an indication for the coil-helix transition of the konjac glucomannan, which takes place in the range of about 60 °C–70 °C [21].

3.2.3. Xanthan-Guar gum mixture

Figure 6 shows the dependency of the storage (G') and loss (G'') moduli on temperature of the guar mixtures with the different xanthan types. In contrast to the measurements of the individual xanthan types and galacto- and glucomannans, the mixtures are not only cooled down from 85 °C to 10 °C, but heated up to 85 °C again after cooling. The curves of the guar gum mixtures with the different xanthan types show very similar trends and behavior. To compare these four systems of the different xanthan gums mixed with guar gum, the gelation point and the storage modulus at a temperature of 25 °C were determined. Since the crossover point of the storage and loss moduli ($G' = G''$) deviated strongly during the cooling process of the XG-GG blends, T_{gel} was determined as the temperature at the inflection point of the G' curve to ensure the reproducibility of the gelation point determination. This point is the one with the highest slope and therefore indicates the highest change in the G'-value [40, 42]. The gelling temperature and storage modulus at 25 °C for the XG-GG compounds are given in table 1. The inflection point of G' is found at similar temperatures between 21.5 °C and 27 °C for the blends. The mixture with XG3 is an exception, as it shows a much earlier inflection point at $T = 26.93$ (±0.29) °C. Furthermore, the guar mixture containing the deacetylated XG3 exhibits the highest G'-value with $G' = 17.97$ (±1.54) Pa, followed by the XG1-GG blends and the mixture with the calcium fermented XG4. The guar mixture containing low-pyruvate XG2 has the lowest G'-value. However, all XG-GG blends show quite a weak increase of the final G'-value at a range of about 30 Pa. This suggests that in all mixtures with guar gum no gelation in the sense of permanent cross-linking takes place, but only an increase in viscosity and moduli.

3.2.4. Xanthan-Locust bean gum mixture

The temperature dependency of the XG-LBG compounds storage and loss moduli are shown in figure 7. The mean values of the locust bean gum mixtures show similar behavior for all xanthan gum types. Furthermore, the gelation curves do not show hysteresis which leads to the conclusion that the cross-linkages responsible for network formation are weak. The results in table 2 can be used to characterize and determine the elastic modulus G' and the gelation temperature of the various xanthan gum mixtures. As the GG blends shown above, the LBG blends with deacetylated XG3 display the highest G' elastic value with $G' = 127.29$ (±20.49) Pa followed by the XG1 blend. The mixtures with pyruvate-poor XG2 and the calcium-fermented xanthan show the lowest G' values. The inflection point of G' of the different XG-LBG compounds ranges between 55 °C and 57 °C for all types of xanthan gum. The gelation during the cooling process thus takes place at a similar temperature for the different XG-LBG mixtures. In contrary to the mixtures with guar gum,

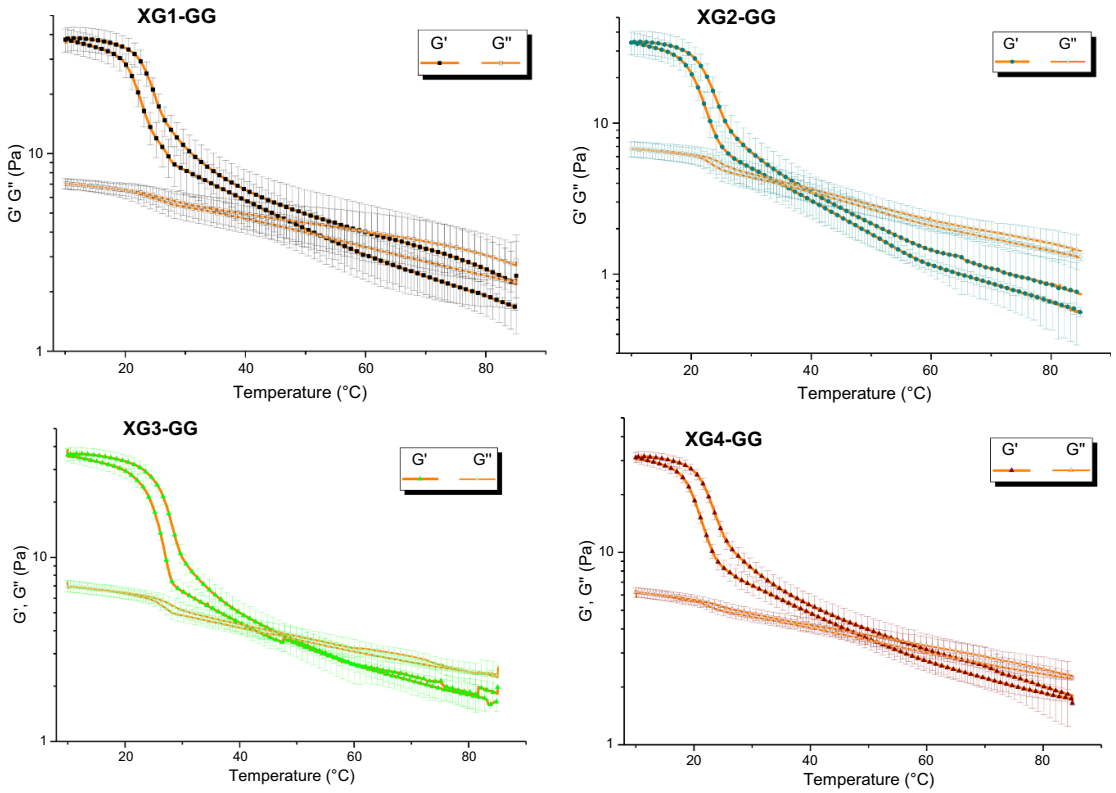

Figure 6. Results of temperature sweeps of 0.5% w/w mixtures of guar gum with the respective xanthan types in the ratio of 20:80 for XG-GG. Logarithmic plot of the average storage and loss moduli G' (filled symbols), G'' (empty symbols) versus temperature at constant frequency ($f = 1$ Hz) and strain ($\gamma = 1$ %).

Table 2. Average of the gelation temperature T_{gel} and storage moduli G' at 25 °C for the XG-LBG blends.

Mixtures	T_{gel} (°C)	SD	G' (Pa) (25 °C)	SD
XG1-LBG	56.90	±1.73	94.01	±2.86
XG2-LBG	55.10	±0.32	83.29	±3.07
XG3-LBG	55.90	±0.02	127.29	±20.49
XG4-LBG	55.6	±1.06	81.94	±6.01

Table 3. Average of the gelation temperature T_{gel} and storage moduli G' at 25 °C for the XG-KGM blends.

Mixtures	T_{gel} (°C)	SD	G' (Pa) (25 °C)	SD
XG1-KGM	63.64	±0.29	420.13	±85.84
XG2-KGM	61.96	±0.5	397.4	±53.23
XG3-KGM	57.91	±0.01	481.84	±60.74
XG4-KGM	62.46	±0.01	359.23	±16.36

the locust bean gum mixtures show gelation for all xanthan gums. The final values of the elastic moduli G' of the LBG mixtures show an increase of about 100–200 Pa compared to guar mixtures.

3.2.5. Xanthan-Konjac glucomannan mixture

Figure 8 shows the storage G' and loss G'' moduli of the various XG-KGM mixtures dependent on temperature. They look similar for all xanthan gum mixtures with konjac glucomannan. In addition, the gelation temperature and storage modulus are given in table 3. Like the GG and LBG blends, the XG3 blend with KGM shows the highest storage modulus $G' = 481.84$ (±60.74) Pa at 25 °C. The following XG-KGM mixtures show the same trend, although more pronounced. The mixture with XG1 displays the second highest G' value, followed by the mixture with the pyruvate-poor XG2 and finally the konjac mixture with the calcium-fermented XG4 that shows the lowest G'. The gelling temperatures of the XG-KGM mixtures are further apart for the different types of xanthan gum than for the XG-GG and XG-LBG mixtures. For the XG3-KGM mixture, gelation occurs at the lowest temperature $T_{gel} = 57.91$ (±0.01) °C and thus at lower

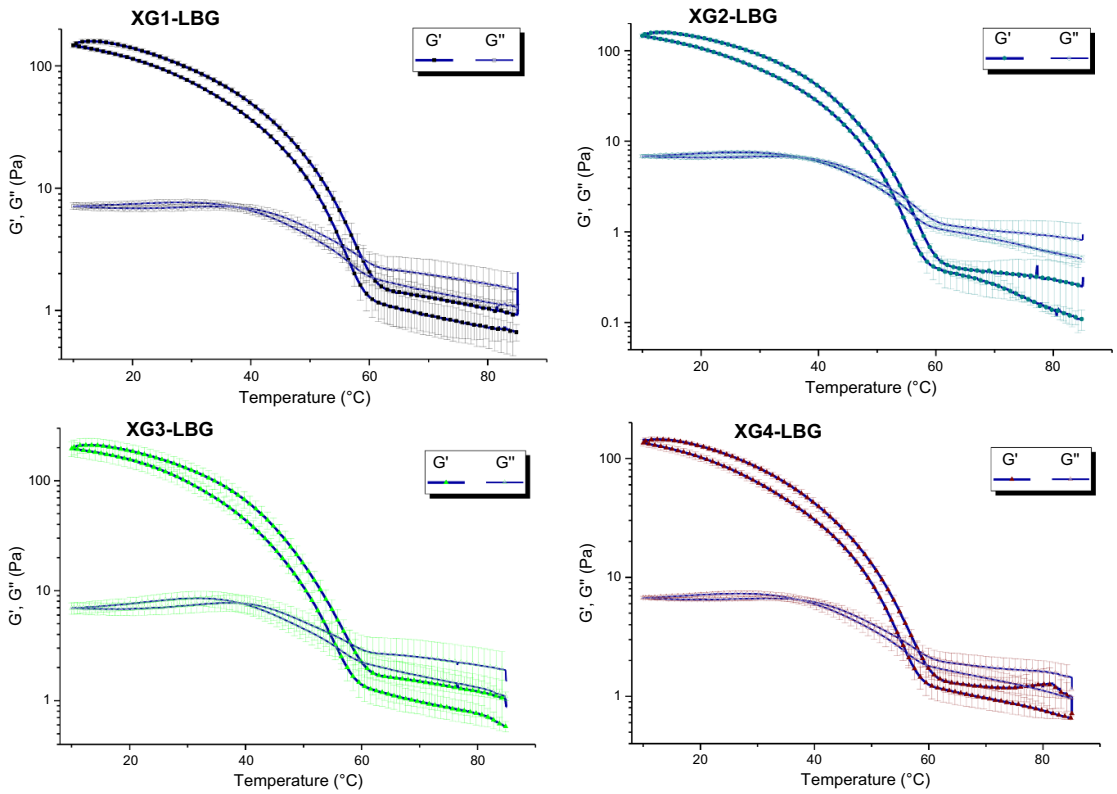

Figure 7. Results of temperature sweep of 0.5% w/w mixtures of locust bean gum with the respective xanthan types in the ratio of 20:80 for XG-LBG. Logarithmic plot of the average storage and loss moduli G' (filled symbols), G'' (empty symbols) versus temperature at constant frequency ($f = 1$ Hz) and strain ($\gamma = 1$ %).

temperatures than for the other XG-KGM mixtures. The KGM mixtures show the highest increase of the final G' -value of approx. 500 Pa at 10 °C compared to the GG and LBG mixtures. The XG-KGM mixtures thus show the strongest gelation for all xanthan types.

3.3. Impact of salt

In order to investigate the influence of salt on the synergistic gelation effects and the gelation mechanisms of the hydrocolloid mixtures, temperature-dependent oscillation measurements were carried out. These were accompanied by measurements of the zeta potential.

3.3.1. Zeta potential

The zeta potential was measured to observe the shielding of the negatively charged xanthan gums dependent on the NaCl concentration. To determine the appropriate salt concentration for the following rheology measurements, XG1 and XG2 were measured representatively for all xanthan types at different NaCl concentration as these are the most salt tolerant of the xanthan gums used in this study. The xanthan gums were measured at a concentration of 0.001% w/w in differently concentrated NaCl solutions (0 mM, 0.1 mM, 0.5 mM, 1 mM, 5 mM, 10 mM, 50 mM, 100 mM, 500 mM). As anionic polyelectrolytes, xanthans show a negative zeta potential. Figure 9 shows a distinct increase in zeta potential with increasing salt concentration for both xanthan gums. With increasing shielding of the negative side chains by the sodium counter ions the xanthan polymers exhibit a zeta potential closer to zero. Additionally, the Debye lengths of the resulting NaCl concentrations were determined to support the zeta potential measurements by taking the xanthan monomer structure into account and estimating the shielding length of the negatively charged side chains.

3.3.2. Xanthan-Guar gum mixture

Figure 10 shows the change of the storage and loss moduli dependent on temperature of the XG-GG mixtures in Milli-Q water without salt as well as with 0.5% w/w (85.56 mM) NaCl and 0.05% w/w (8.56 mM) NaCl. It can be seen that with increasing salt concentration the moduli and thus also the synergism of the mixtures decrease.

In order to illustrate the effect of salt on the temperature dependence of the viscoelastic properties, the temperature sweep measurements previously shown, in which samples only included Milli-Q water and no

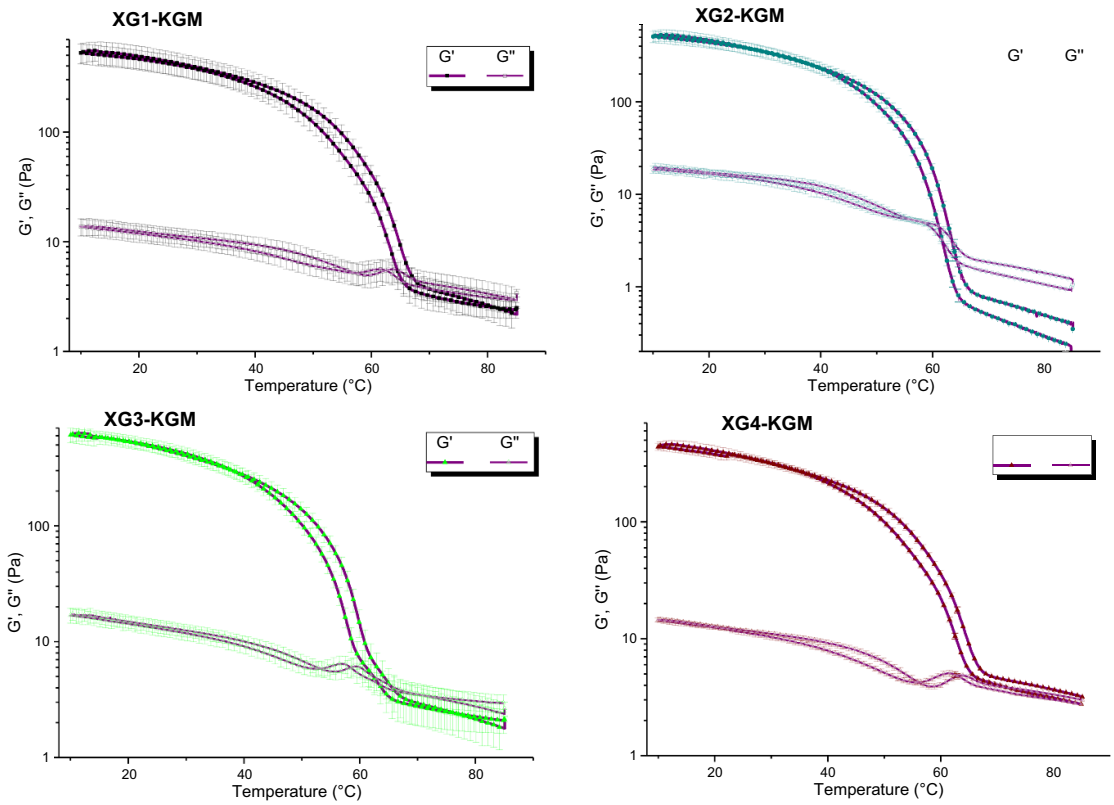

Figure 8. Results of temperature sweeps of 0.5% w/w mixtures of konjac glucomannan with the respective xanthan types in the ratio of 60:40 for XG-KGM. Logarithmic plot of the average storage and loss moduli G′ (filled symbols), G″ (empty symbols) versus temperature at constant frequency ($f = 1$ Hz) and strain ($\gamma = 1$ %).

Table 4. Average of the gelation temperature T_{gel} and storage moduli G' at 25 °C for the XG-GG blends with 0 %, 0.05% and 0.5% w/w NaCl.

	0% w/w NaCl		0.05% w/w NaCl		0.5% w/w NaCl	
Mixture	T_{gel} (°C)	G' (Pa) (25 °C)	T_{gel} (°C)	G' (Pa) (25 °C)	T_{gel} (°C)	G' (Pa) (25 °C)
XG1-GG	22.54 ± 0,51	12.06 ± 2.41	23.25 ± 0.00	4,20 ± 1.56	–	5.02 ± 0.48
XG2-GG	22.53 ± 0.49	7.03 ± 1.84	23.03 ± 0.00	1.63 ± 0.29	–	2.55 ± 0.15
XG3-GG	26.93 ± 0.29	17.97 ± 1.54	26.58 ± 0.01	9.10 ± 1.06	–	5.13 ± 0.63
XG4-GG	21.53 ± 0.51	8.33 ± 0.82	21.78 ± 0.00	5.02 ± 0.68	–	6.73 ± 0.21

salt, are again displayed for comparison. The curves clearly visualize that the guar mixtures with salt for all types of xanthan gums no longer show an increase in the storage modulus G' at about 20 °C–30 °C by lowering the temperature. In addition, it can be seen from table 4 that the storage moduli G' of the guar gum mixtures for all xanthan types are significantly lower compared to the mixtures without salt. Furthermore, no inflection point could be determined for the higher salt concentration of 0.5% w/w.

3.3.3. Xanthan-Locust bean gum mixture

In figure 11, the gelation curves of the XG-LBG mixtures in Milli-Q water without salt as well as with salt are shown. The mixtures with salt show a reduction of the final moduli compared to the mixtures without salt, whereas the gelation point hardly differs from the mixtures without salt. Up to the beginning of gelation the curves of the different systems are similar and a discrepancy can be observed once the inflection point has been reached. While the locust bean gum mixture with the deacetylated XG3 in Milli-Q water shows the highest synergism and a storage modulus of $G' = 127.29$ ($\pm$20. 49) Pa, the G' -value of the mixture in 0.5% w/w NaCl solution is only $G' = 34.39$ Pa ($\pm$1.27) Pa. For further interpretation, the gelation temperature and G' at 25 °C can be compared from table 5.

3.3.4. Xanthan-Konjac glucomannan mixture

Figure 12 shows the gelation curves of the different xanthan gum mixtures with konjac glucomannan in Milli-Q water without salt as well as with salt and reveals two distinct characteristics: with salt, the mixtures

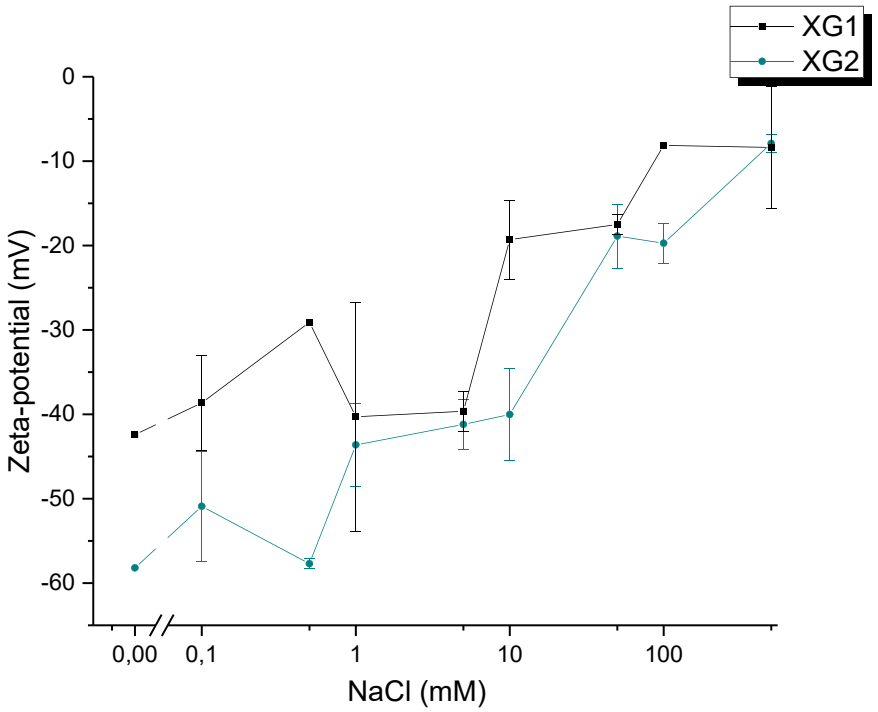

Figure 9. Zeta potential of 0.001%w/w xanthan gum solutions as a function of NaCl concentration. The absolute value of the zeta potential increases with increasing salt concentration as the shielding of the negatively charged xanthan gum is increased.

Table 5. Average of the gelation temperature T_{gel} and storage moduli G' at 25 °C for the XG-LBG blends with 0 %, 0.05% and 0.5% w/w NaCl.

	0% w/w NaCl		0.05% w/w NaCl		0.5% w/w NaCl	
Mixture	T_{gel} (°C)	G' (Pa) (25 °C)	T_{gel} (°C)	G' (Pa) (25 °C)	T_{gel} (°C)	G' (Pa) (25 °C)
XG1-LBG	56.9 ± 1.73	94.01 ± 2.86	54.71 ± 0.56	55.38 ± 2.69	57.40 ± 0.89	39.01 ± 3.27
XG2-LBG	55.1 ± 0.32	83.29 ± 3.07	53. 35 ± 0.89	44.34 ± 1.47	53.87 ± 1.02	22.78 ± 4.06
XG3-LBG	55.9 ± 0.02	127.29 ± 20.49	54.37 ± 0.01	75.10 ± 6.28	59.42 ± 0.87	34.39 ± 1.27
XG4-LBG	55.6 ± 1.06	81.94 ± 6.00	53.68 ± 0.59	43.19 ± 1.55	55.56 ± 0.6	28.03 ± 1.17

Table 6. Average of the gelation temperature T_{gel} and storage moduli G' at 25 °C for the XG-KGM blends with 0 %, 0.05% and 0.5% w/w NaCl.

	0% w/w NaCl		0.05% w/w NaCl		0.5% w/w NaCl	
Mixture	T_{gel} (°C)	G' (Pa) (25 °C)	T_{gel} (°C)	G' (Pa) (25 °C)	T_{gel} (°C)	G' (Pa) (25 °C)
XG1-KGM	63.64 ± 0.29	420.13 ± 85.84	60.95 ± 0.89	284.23 ± 26.56	48.99 ± 0.28	107.38 ± 4.36
XG2-KGM	61.96 ± 0.5	397.40 ± 53.23	59.76 ± 0.29	257.18 ± 26.34	47.98 ± 0.77	93.73 ± 1.58
XG3-KGM	57.91 ± 0.01	481.84 ± 60.74	56.05 ± 0.58	313.01 ± 10.32	53.19 ± 0.29	117.10 ± 7.06
XG4-KGM	62.46 ± 0.01	359.23 ± 16.36	60.61 ± 0.79	221.98 ± 3.73	47.13 ± 0.29	110.41 ± 16.5

now show a very strong reduction of the end moduli. Furthermore, there is a clear shift in the gelation towards lower temperatures. Comparison of the synergism of the blends with the deacetylated XG3 points out the strong salt influence on the gel strength. In pure Milli-Q, the XG3-KGM mixtures show a storage modulus of $G' = 481.81$ Pa (±60.74), whereas in a 0.05% w/w NaCl solution the moduli decrease to $G' = 313.01$ Pa (±10.32) and with 0.5% w/w NaCl even down to $G' = 117.1$ Pa (±7.06). The gelation temperature and the storage modulus at 25 °C of the konjac mixtures in a 0.5% w/w NaCl solution are listed in table 6.

3.4. Discussion

The following section discusses the gelation mechanisms and explains the interaction of the xanthan gum types with the galacto- and glucmannan, thus their different synergies. However, the curves are discussed exemplarily and therefore only one measurement with a xanthan gum and the respective GG, LBG and KGM mixtures are shown. Furthermore, the model is presented and for a better understanding the

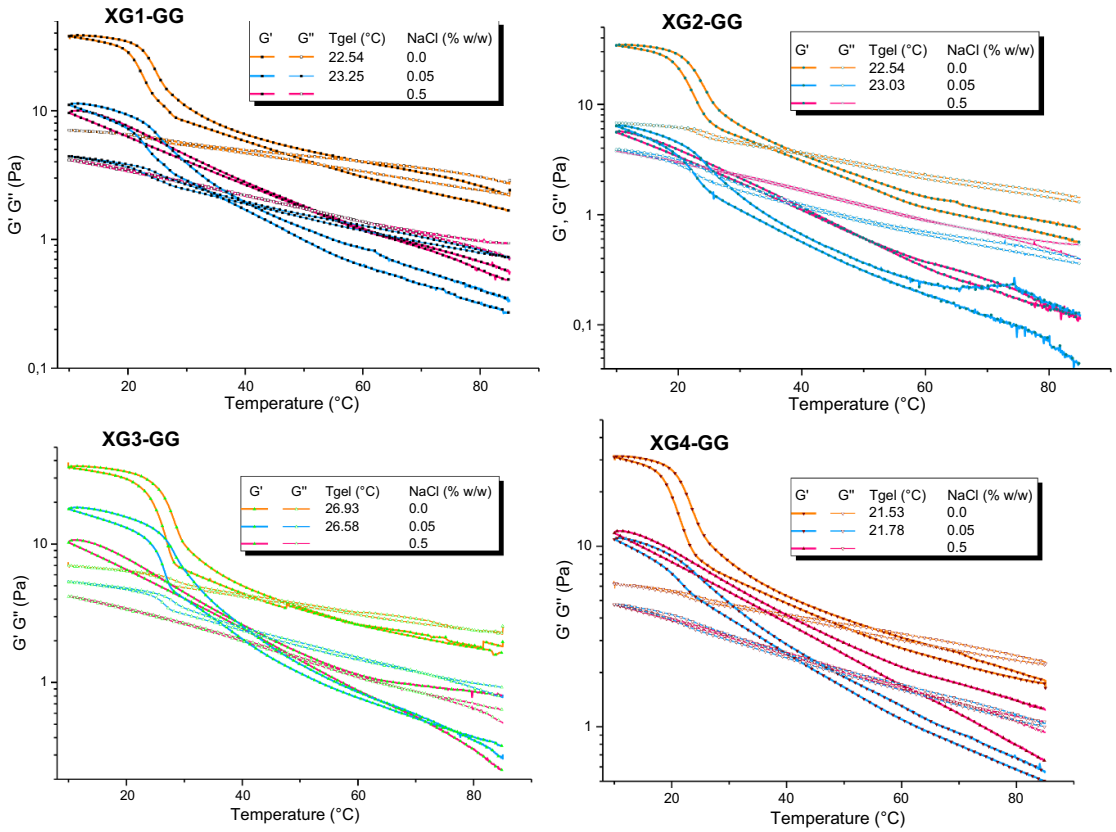

Figure 10. Results of temperature sweep of 0.5% w/w mixtures of guar gum with the respective xanthan types in the ratio of 20:80 for XG-GG in Milli-Q water without salt as well as with 0.05% and 0.5% w/w NaCl added. Logarithmic plot of the average storage and loss moduli G′ (filled symbols), G″ (empty symbols) versus temperature at constant frequency ($f = 1$ Hz) and strain ($\gamma = 1$ %). For the sake of clarity, error bars have been omitted.

temperature-dependent behavior of the different mixing systems and the arrangement of the molecules are discussed by means of a schematic representation.

3.4.1. Gelation mechanisms of xanthan and galacto- glucomannan.

3.4.1.1. Xanthan-Guar gum mixture

Figure 13 shows the temperature-dependent development of storage G' and loss G'' moduli for the XG-GG mixture. At high temperatures a strong temperature-induced mixing takes place at $T > T_{gel}$. The increase in temperature is the added energy that accelerates the fast flexible guar molecules and greatly increases the overall mixing of the system.

When cooling, the thermal energy decreases, resulting in weaker movements and slower dynamics of the xanthan gum molecules and especially the flexible guar molecules. These large scale effects ruled by entropy driven demixing are due to the different dynamics of the molecules and their flexibility. Furthermore, the helix transition of the xanthan molecules occurs at relatively high temperature (~40 °C), and hence still under good mixing condition. In addition, the numerous side chains and the flexibility of guar gum make interaction with xanthan more difficult.

As the temperature decreases further, the stiff negatively charged xanthan gum molecules 'freeze' due to the restricted movement caused by the strong repulsion of the surrounding molecules at random positions with random orientation and undergo a so-called 'jamming transition' [10, 41]. However, the arrangement of the highly dynamic flexible guar molecules between the immobilized rigid and randomly oriented rod-like xanthan molecules is entropically unfavorable and entropically driven phase separation occurs. This inhomogeneous mixture now has an increased local concentration, within its phases, which shows an effective increase of modulus of respective phases. Such observation of domain formation is also called the filling effect [6]. The modulus increase thus results from a phase separation induced domain formation and not from gelation due to the formation of physically permanent networks. Furthermore, the increase of modulus is supported by formation of hydrogen bonds, which due to their weak interaction only occur at low thermal energy around 25 °C, and correspondingly slower dynamics of the guar molecules. Hydrogen bonds can also be formed at the domain interfaces between the guar gum and xanthan phases.

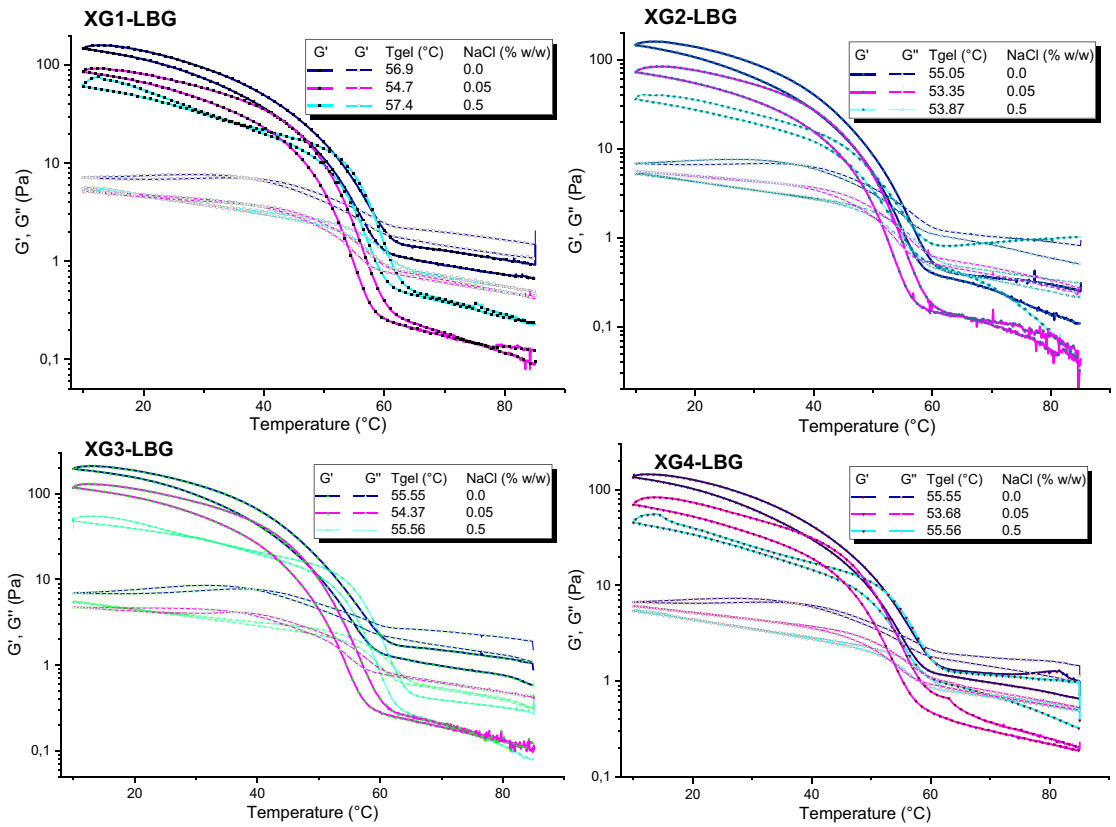

Figure 11. Results of temperature sweep of 0.5% w/w mixtures of locust bean gum with the respective xanthan types in the ratio of 20:80 for XG-LBG in Milli-Q water without salt as well as with 0.05% and 0.5% w/w NaCl added. Logarithmic plot of the average storage and loss moduli G′ (filled symbols), G″ (empty symbols) versus temperature at constant frequency ($f = 1$ Hz) and strain ($\gamma = 1$ %). For the sake of clarity, error bars have been omitted.

The moduli increase can be explained by the following: The jamming of xanthan molecules, which already occurs at higher temperatures, domain formation by phase separation, entanglements in the guar gum domains and the formation of hydrogen bonds both in the guar gum domain and at the domain interface between the xanthan gum and guar gum phases.

3.4.1.2. Xanthan-Locust bean gum mixture

Figure 14 shows the temperature dependent development of storage G' and loss G'' moduli for the XG-LBG mixture. In this case a new effect appears compared to the XG-GG mixture. The high moduli of the XG-LBG mixture indicates gelation. In addition, a reversible network formation can be noted, since the curves do not show any thermal hysteresis of the moduli between cooling and heating process. As already explained, this means that the energy of bond formation and that of the unbinding is the same and there exist 'weak' interactions that do not require much energy to dissolve. The absence of hysteresis confirms the assumption that xanthan molecule forms a helix that requires very low energy for the coil-helix transition. When reheating, the xanthan single helix is easily wound up.

This observation leads to the following model. As already mentioned, the xanthan undergoes a conformational change from a disordered shape at high temperature to a rigid ordered helix structure at low temperature. Previous studies assumed that an intermolecular bond between the xanthan in its coil conformation and the galactomannan occurs [23]. We propose that, when cooling the previously heated XG-LBG mixtures, the xanthan molecule traps the LBG at its helix transition and forms the weak (cross-links) network. In comparison, guar gum as a fast and highly flexible molecule is not wound by xanthan. In addition, the high number of GG side chains impede the helical winding due to steric hindrance. The short, semi-flexible locust bean gum with its lower mobility has a lower tendency to phase separation with the stiff xanthan gum. The LBG molecules are less flexible, which increases the probability of 'capture'. Furthermore, the lower number of side chains leads to less steric hindrance.

As can be seen in figure 14, all this contributes to the fact that when the xanthan molecules change their conformation, the LBG is trapped in the helix structure and the interaction between the two takes place. The helical winding forms the junction zones (cross-links) of the gel network and leads to a pronounced increase

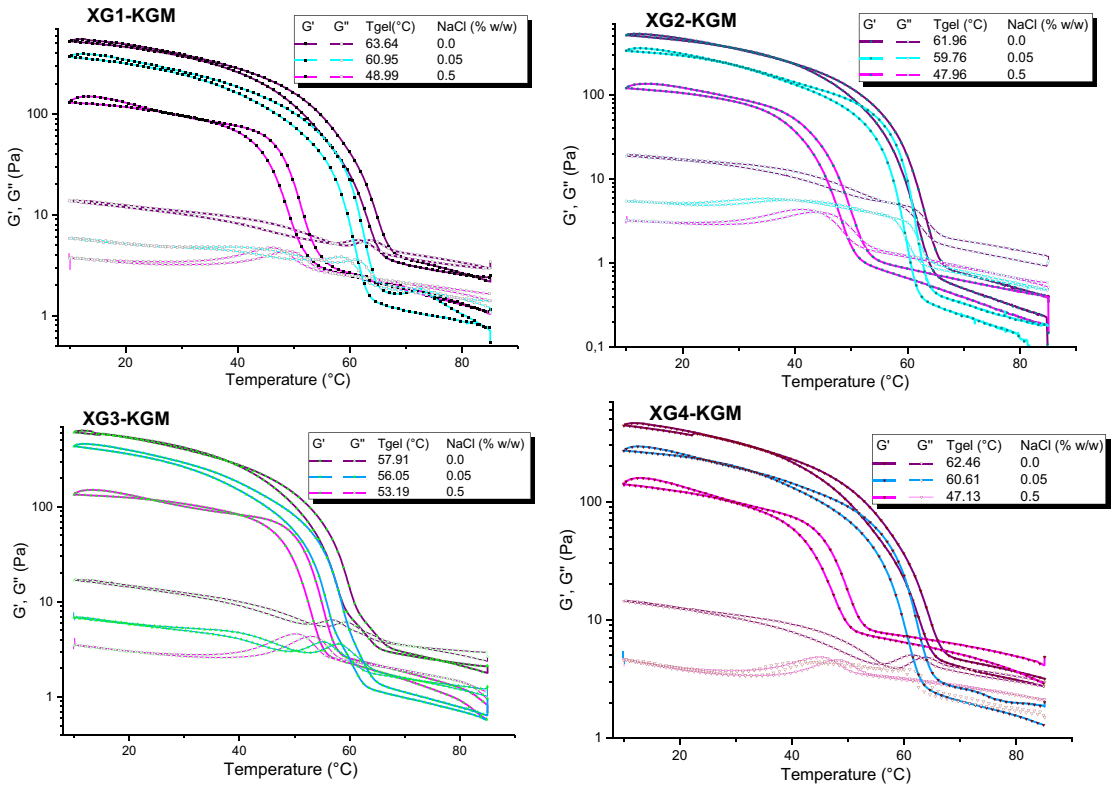

Figure 12. Results of temperature sweep of 0.5% w/w mixtures of konjac glucomannan with the respective xanthan types in the ratio of 20:80 for XG-KGM in Milli-Q water without salt as well as with 0.0 5% and 0.5% w/w NaCl added. Logarithmic plot of the average storage and loss moduli G′ (filled symbols) G″ (empty symbols) versus temperature at constant frequency ($f = 1$ Hz) and strain ($\gamma = 1$ %). For the sake of clarity, error bars have been omitted.

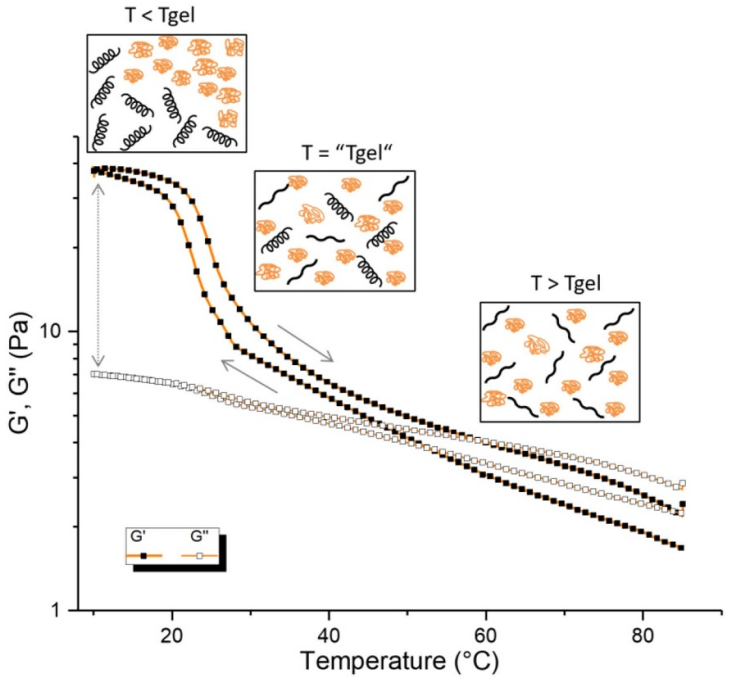

Figure 13. Temperature dependency of 0.5% w/w xanthan gum-guar gum mixture in the ratio of 20:80 for XG-GG. Logarithmic plot of the average storage and loss moduli G′ (filled symbols), G″ (empty symbols) versus temperature at constant frequency ($f = 1$ Hz) and strain ($\gamma = 1$ %). Schematic illustration of XG and GG in the mixture during the cooling process. GG as a flexible orange twined structure and XG at high temperature still as a black flexible rod, which undergoes the coil-helix transition during cooling.

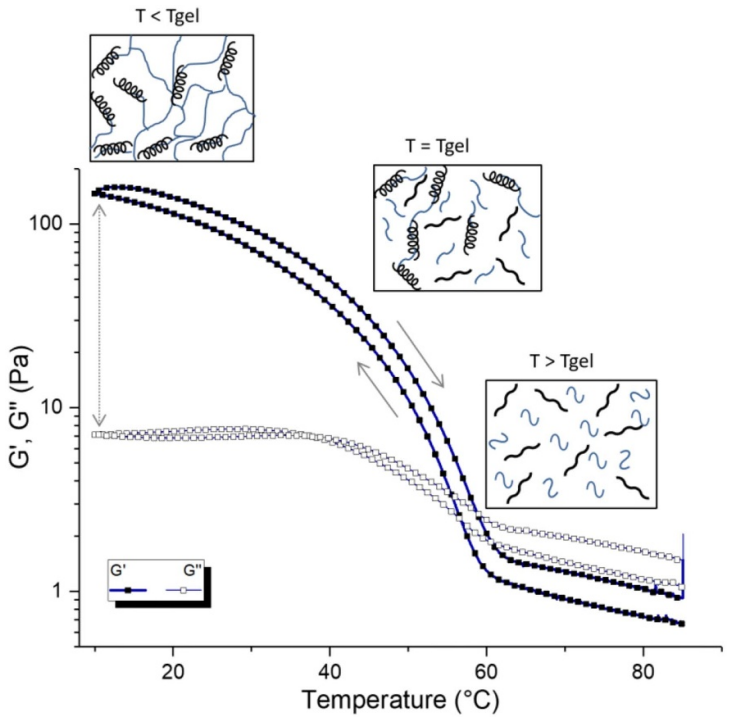

Figure 14. Temperature dependency of 0.5% w/w of xanthan gum-locuust bean gum mixture in the ratio of 20:80 for XG-LBG. Logarithmic plot of the average storage and loss moduli G' (filled symbols), G'' (empty symbols) versus temperature at constant frequency ($f = 1$ Hz) and strain ($\gamma = 1$ %). Schematic illustration of XG and LBG in the mixture during the cooling process. LBG represented as a semi-flexible rod, which is helically coiled by XG during gelation and leading to a network. XG is represented as a black flexible rod, which takes the helix-conformation during cooling.

in synergism. Thus, the modulus increase results from intermolecular interaction by helical winding. The fact that these weak cross-links can be quickly dissolved when the temperature increases is indicated by the small hysteresis.

3.4.1.3. Xanthan-Konjac glucomannan mixture

The temperature dependent development of G' and G'' of the XG-KGM mixture shows gelation that indicates reversible network formation, as seen in figure 15. It also shows no thermal hysteresis due to weak interactions of the network structure, which require low energy for their dissolution. No cooperative movements are necessary, as they are required when winding up intertwined double helices. The nonexistence of hysteresis can be explained by the fact that the transition of the single helix of xanthan quickly changes into its coiled form when the mixture is reheated. However, two significant differences can be observed in contrast to LBG-XG mixture. Firstly the final G' modulus is much higher and secondly the gelation already starts at a markedly higher temperature of approx. 60 °C (with XG-LBG it is around 55 °C). An important aspect to mention is that KGM, undergoes a coil-helix transition at approx. 60 °C (see figure 5(b)).

This means that the konjac helix transition takes place at higher temperature and thus earlier during the cooling process compared to the coil helix transition of xanthan. This leads to the assumption that while temperature reduction, konjac winds around the chain ends of the stiff rod-like and dynamically slow xanthan by helical formation. The modulus increase here results due to an intermolecular interaction by helical winding. Especially the observed measurements of the KGM mixtures, which show marked differences compared to the LBG mixtures, reveal that indeed different gelation mechanisms take place between the two mixtures

3.4.2. Maximum synergism of the different mixtures

The viscoelastic properties and synergy effects for the different galacto- and glucomannan systems shown in figure 3 can now be explained with the proposed model of the different gelation mechanisms described above. The small modulus increase, thus the weak synergism of the XG-GG mixture is mainly due to phase separation. The XG-LBG mixtures show a stronger synergy effect through network formation, as the cross-links are formed by xanthan gum connected by LBG. Finally, a very strong synergy effect can be observed with KGM mixtures. In this case the cross-links are formed by konjac which are connected by

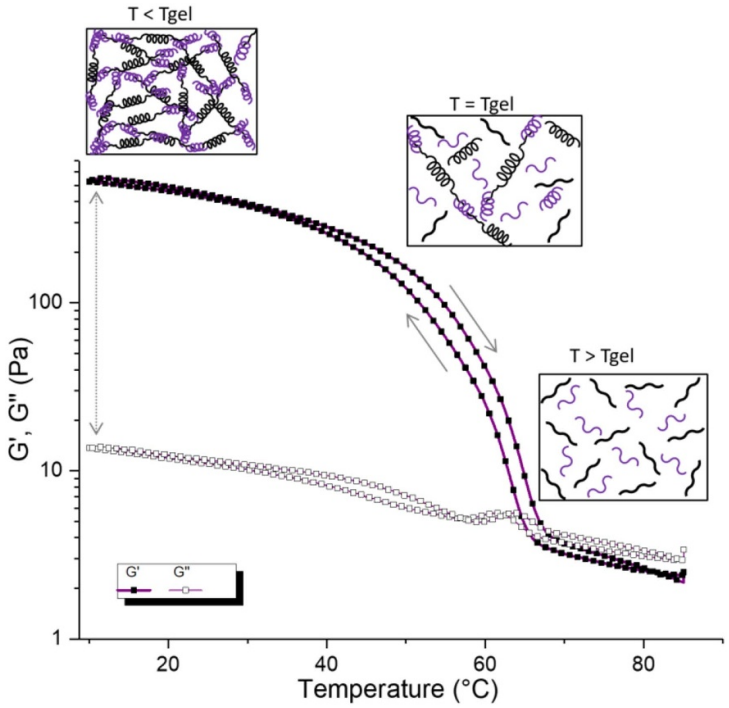

Figure 15. Temperature dependency of 0.5% w/w of xanthan gum-konjac glucmannan mixture in the ratio of 60:40 for XG-KGM. Logarithmic plot of the average storage and loss moduli G' (filled symbols) G'' (empty symbols) versus temperature at constant frequency ($f = 1$ Hz) and strain ($\gamma = 1$ %). Schematic illustration of XG and KGM in the mixture during the cooling process. KGM represented at high temperature as violet semi-flexible rod, which forms a helix-conformation while cooling and winds around the chain ends of the dynamically slow XG by helix formation. XG is represented as a black flexible rod, which also takes the helix-conformation during cooling, helically coiled by KGM during gelation and leading to a network.

xanthan. The higher maximum of XG-KGM mixture compared to the XG-LBG mixture can be explained by the fact that the xanthan as a molecule between the cross-links, which form the mesh, is stiffer than the LBG (see figure 15 illustration at $T > T_{gel}$). If the xanthan molecule no longer acts as a cross-link but as a molecule that forms the mesh, it increases the resistance of the whole system as a stiff molecule (compared to more flexible molecule) and thus the elastic modulus.

Figure 16 shows how the synergism differs when using the individual types of xanthan gum. It can be seen mixtures for the ratios, displaying the highest storage modulus G' resulting from the amplitude sweeps shown in figures 4(a)–(c). For illustration also the individual components are plotted. As already indicated in figures 4(a)–(c) the mixture with XG3 exhibits the highest storage modulus for all blend systems. The other types of xanthan show no significant differences in the elastic modulus. The increase in G' modulus of XG3 > XG1 > XG4 > XG2 for XG-GG mixtures can be explained by the increasing molecular weight and thus is dominated by xanthan gum. However the storage modulus increase of the XG3 mixture with LBG and KGM, cannot be explained by the molecular weight of the xanthan gum but by the fact, that XG3 contains less number of acetate groups. According to current insight, the acetate groups of the non-terminal mannose side chains of the xanthan stabilize its helix structure by intramolecular hydrogen bonding. It has been reported that less acetate groups enhanced the synergism with galacto- and glucomannan mixtures [24]. Furthermore, it was shown, that modifications of deacetylation destabilized the helix structure of the xanthan leading to enhanced synergistic gelation of xanthan and mannan mixture [7, 43, 44]. In addition, Tako *et al* [7, 45] determined that the xanthan structure became more flexible after deacetylation and thus the coil-helix transition was less pronounced. The flexibility of the XG3 promotes the interaction with the flexible guar gum molecule, leading to more entanglement and higher modulus. Tako *et al* assumed, that the helix conformation of xanthan molecule takes place via van der Waals interaction between the methyl group of the acetyl residue of the mannose side chain and the oxygen of the hemiacetal in the glucose backbone [29].

The strong modulus increase of the LBG and KGM mixtures with XG3 can be explained by the fact that fewer acetyl groups destabilize the helix structure of xanthan. The lower number of acetyl groups leads to a deceleration of the helix transition during cooling, as the helix is less stable due to the absence of acetyl group and thus less interaction. Consequently, more time remains for the LBG winding of the xanthan by cause of the slowed helix transition. Thus more LBG molecules are wound during the entire gelling process, resulting in more cross-links and a tighter and denser network.

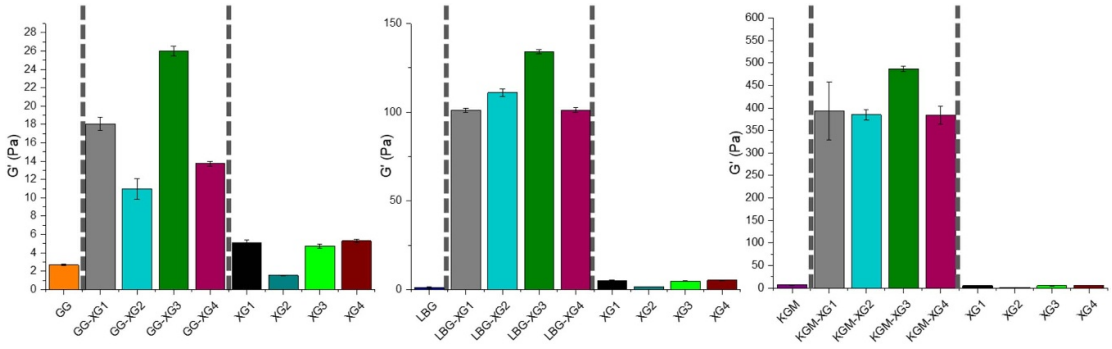

Figure 16. Storage modulus of the 0.5% w/w single components and blends of XG-GG and XG-LBG in the ratio 20:80 and XG-KGM in the ratio 60:40. The mean values of the modulus were taken from the amplitude sweep at a deformation of $\gamma = 1$ %. Frequency ($f = 1$ Hz) and temperature ($T = 25$ °C) are constant.

In the case of KGM, the decelerated helix formation of XG3 results in its longer availability in its disordered coil form for the coil-helix transition of konjac. As a result more xanthan molecules are captured by konjac at its helix transition. Due to the increased XG inclusion by konjac, more cross-links are formed, which also leads to a tighter and denser network, which in turn cause the increase of the elastic modulus. The assumption that konjac traps xanthan more easily in its disordered coil form is apparent from the observed temperature sweep. The gelation of XG-KGM mixtures occurs before the coil-helix transition of xanthan gum and supports the conclusion that the XG3 inclusion of KGM takes place while XG3 is not yet present in its helix form. These observations are in accordance with previous studies, which were obtained by rheology measurements, x-ray structure analysis and optical rotation measurements [34, 46].

3.4.3. Salt impact on xanthan and galacto-, glucomannan mixture

The following discusses the influence of salt on the gelling mechanism, respectively the interaction of the hydrocolloid mixtures, on the basis of the previously proposed models. Therefore the temperature sweep for the galacto- and glucomannan mixing systems in 0.5% w/w NaCl are shown. For illustration of the salt influence on the temperature dependence of the viscoelastic properties, the previously shown temperature sweep of the respective mixtures in Milli-Q water are shown for comparison.

3.4.3.1. Salt impact on xanthan-guar gum mixture

Figure 17 shows the temperature dependent behavior of XG-GG mixture with 0.5% w/w NaCl. It can be clearly seen that the curve shows no increase with temperature. As explained above, when mixing in Milli-Q water, the storage modulus (G') increase is due to phase separation. Hence, in presence of salt an extreme reduction in modulus takes place and the entire temperature-dependent curve changes significantly. Because of the salt, the negatively charged xanthan side chains, which repel each other due to coulomb interactions, are shielded by the cations. Although the helix formation becomes weaker, the molecule still remains stiff because of the side chains. The shielding allows the xanthan molecules to come closer together, leading to a weak jamming. However, the uncharged guar gum molecules, not affected by salt, still have the tendency to phase separate. Demixing also happens in the presence of salt, but does not raise the modulus by virtue of the weak repulsion of xanthan molecules.

3.4.3.2. Salt impact on xanthan-locust bean gum mixture

Temperature dependent behavior of XG-LBG with 0.5% w/w NaCl shown in figure 18 exhibits a lower final modulus. But compared to the XG-GG mixture however, the whole shape of the curve changes less when salt is added. The temperature at which gelation starts is approximately the same for XG-LBG with and without salt, implying by adding salt no shift in the gelling temperature. This can be explained by the fact that the uncharged polar LBG undergoes no structural change with temperature and therefore cannot influence the gel point. Additionally, the shielding of the negatively charged xanthan side chains, the reduced coulomb interaction and thus the repulsion between them leads to an impaired helix formation and helical winding of the LBG molecules by XG. This in turn leads to a weakened helical winding, weak cross-links of xanthan molecules are formed, which allow the LBG molecules to slide out more easily. Thus, due to fewer cross-links, the network is weaker, causing a reduction of the final modulus.

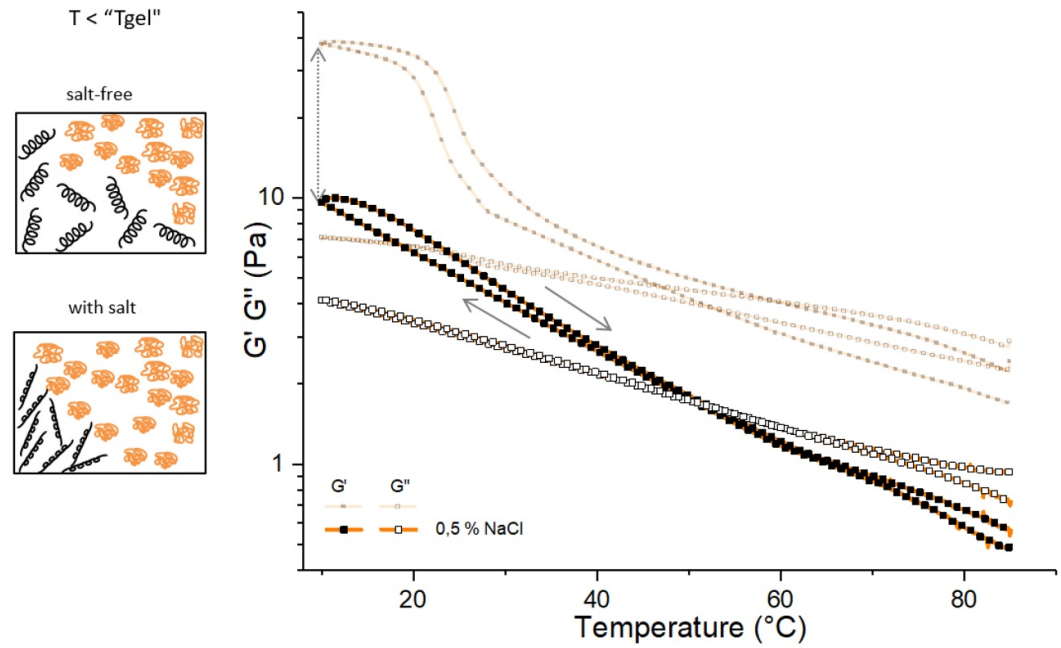

Figure 17. Temperature dependency of 0.5% w/w xanthan-guar gum mixture (20:80 for XG-GG) with 0.5% w/w NaCl and with Milli-Q water for comparison. Logarithmic plot of the average storage and loss moduli G′ (filled symbols), G″ (empty symbols) versus temperature at constant frequency ($f = 1$ Hz) and strain ($\gamma = 1$ %). Schematic illustration of GG, as flexible orange twined structure and XG in a more flexible helix structure (black), showing a strong decrease in modulus in the presence of salt at low temperature due to the weak XG jamming transition. For comparison, the illustration without salt is also shown.

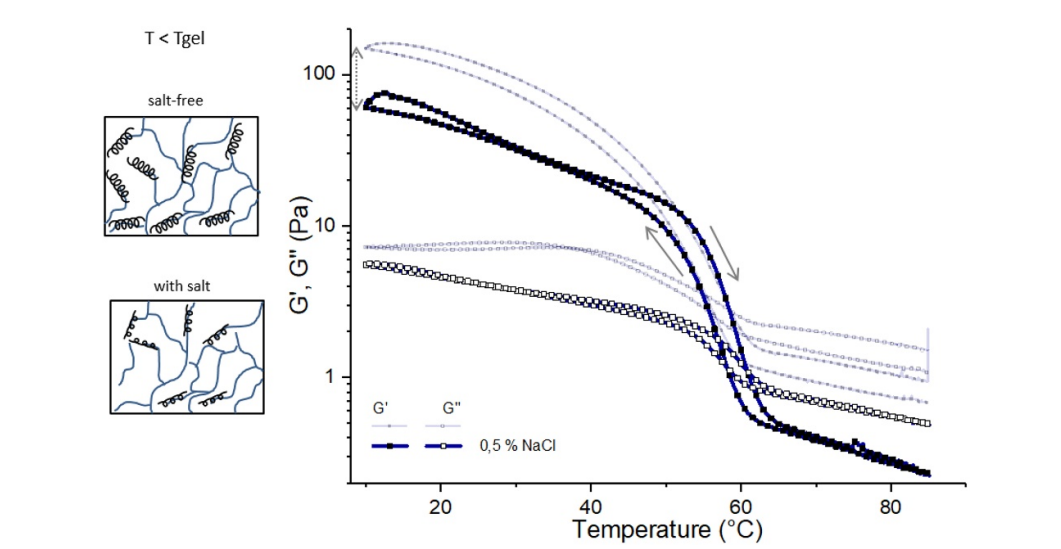

Figure 18. Temperature dependency of 0.5% w/w of xanthan gum-locust bean gum mixture (20:80 for XG- LBG) with 0.5% w/w NaCl and with Milli-Q water for comparison. Logarithmic plot of the average storage and loss moduli G′ (filled symbols), G″ (empty symbols) versus temperature at constant frequency ($f = 1$ Hz) and strain ($\gamma = 1$ %). Schematic illustration of XG and LBG in the mixture in gel state in the presence of salt. Negatively charged xanthan molecules shielded by salt form weak cross-links. Due to impaired helical winding of LBG molecules (blue) by XG (black) a weakened gel network is formed and a reduced storage modulus G′ results. For comparison, the illustration without salt is also shown.

3.4.3.3. Salt impact on xanthan-konjac gum mixture

Besides a very significant decrease in modulus, a clear shift of the gelation towards low temperature can be seen in figure 19, resulting from the temperature sweep of the xanthan-konjac glucomannan mixture with 0.5% w/w NaCl. Due to shielding of negatively charged side chains and the resulting lower coulomb interaction, repulsion is reduced. Helix formation is impaired and leads to more flexible and less rigidly ordered xanthan molecules. The more flexible xanthan gum forms the connection between the konjac, which in turn acts as cross-links in the gel network, consequently leads to a reduction in modulus due to the weaker network structure. Furthermore the shift in gelation suggest that the salt also influence konjac. Water, bound by the salt through hydrate shell, is no longer available for helix formation of the konjac. As a consequence,

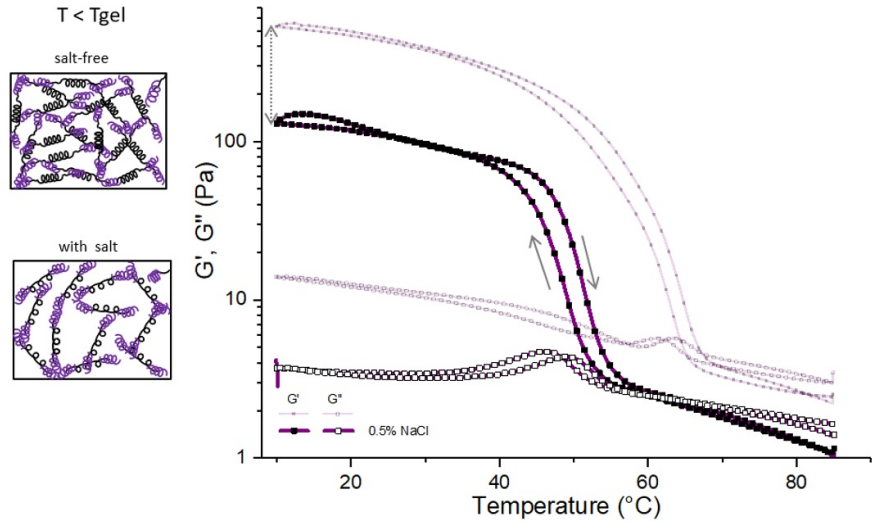

Figure 19. Temperature dependency of 0.5% w/w of xanthan gum-konjac glucomannan mixture (60:40 for XG- KGM) with 0.5% w/w NaCl and with Milli-Q water for comparison. Logarithmic plot of the average storage and loss moduli G′ (filled symbols), G″ (empty symbols) versus temperature at constant frequency ($f = 1$ Hz) and strain ($\gamma = 1$ %). Schematic illustration of XG and KGM in the mixture in gel state in the presence of salt. Negatively charged XG molecules (black) shielded by salt form more flexible connections between the KGM cross-links (violet). This formation of a weaker network structure leads to a reduction of the storage modulus G′. Furthermore, the presence of salt leads to a shift of the gelation temperature to lower temperatures. For comparison, the illustration without salt is also shown.

the helix formation of the konjac shifts to lower temperature, since the intramolecular interactions of the konjac predominate. Furthermore, the less pronounced jamming and the increase in dynamics of the xanthan molecules as a result of the reduced repulsion between those, lead to a delay in the helical winding of xanthan by konjac, since xanthan immobilized at lower temperature. Hence, gelation point shifts to lower temperature.

4. Conclusion

In this work, we have investigated the different heat induced synergistic gelation effects of mixtures of different types of xanthan gum with guar gum, locust bean gum and konjac glucomannan and proposed physicochemical models explaining the underlying molecular mechanisms. Oscillatory measurements including amplitude and temperature sweeps were performed to obtain information about the viscoelastic properties and gelation mechanisms influenced by the physicochemical properties and molecular characteristics of the different hydrocolloids. It is shown that the synergistic gelation effect mainly depends on the flexibility, chain stiffness and side chains of the polymers as well as to a lesser extent on the molecular weight.

The highest synergistic effect occurs in mixtures of xanthan gum with konjac glucomannan, followed by xanthan gum-locust bean gum mixtures, while mixtures of xanthan gum with guar gum show only a slight synergism, not even resulting in firm gels at any mixing ratio. Entropy driven phase separation in the latter system due to the large difference in molecular flexibility prevents effective gel formation and small increase in moduli can be attributed to a filling effect due to the increased local concentration after phase separation. In the case of mixtures with the less flexible LBG molecules which also possess fewer side chains, phase separation is less favorable and LBG can be trapped by xanthan undergoing a coil-helix formation upon cooling, thus resulting in a cross-linked network. A similar process is proposed for xanthan gum-konjac glucomannan mixture. However, since konjac also undergoes a coil to helix transition at higher temperature than xanthan, it is likely that konjac in this case traps xanthan molecules during cooling, resulting in a network with even higher elasticity due to the high stiffness of xanthan molecules forming the mesh between the konjac cross-links.

For all galacto- and glucomann mixed systems, the highest elastic modulus and thus the highest synergism within the types of xanthan was observed for mixture with deacetylated XG3.This can be explained by molecular weight on the one hand and by lower number of acetyl residues on the other hand, leading to a less stable helix structure. The less pronounced helix transition promotes the interaction with the mannan and thus a higher modulus.

Addition of sodium chloride induces changes in gelation mechanisms and reduction in synergism in all systems. Shielding of the negatively charged side chains of xanthan results in a reduction of coulomb repulsion, allowing the xanthan molecule to come closer and undergo a weaker jamming transition. Furthermore, an impaired helix formation and helical winding of the LBG molecule by XG arise. This in turn leads to weaker cross-links and a looser gel network respectively, thus a reduction in modulus. In case of XG-KGM, the shielded and more flexible xanthan molecule leads to a reduction in modulus due to looser network structure. Moreover, the gelation point is shifted to a lower temperature by adding salt. This results from a competition between the salt and KGM for available water to form hydration shells, leading to a destabilized helix formation. Additionally, the less pronounced jamming and the increase in dynamics of the xanthan molecules as a result of the reduced repulsion between them leads to a delay in the helical winding of xanthan by konjac, since xanthan is immobilized at lower temperature. Hence, the gelation point shifts to a lower temperature.

Combining the findings presented here, this study demonstrates the synergistic gelation effects of non-gelling thickeners in combination with other non-gelling thickeners and the detailed gelation mechanism between them. These findings can thus contribute to broaden the scope of application of mixtures of non-gelling hydrocolloids.

Acknowledgments

The authors would like to thank Jungbunzlauer Ladenburg GmbH, Dr. Albert-Reimann-Strasse 18, 68526 Ladenburg, Germany for funding this study. Many thanks go to Dr Kaloian Koynov and especially Andreas Hanewald for the technical support during rheometer experiments. Furthermore we thank the members of the MPIP soft matter food science group for fruitful discussion and proofreading the manuscript.

Funding:

This work was supported by the company Jungbunzlauer (Ladenburg, Germany) by financing Marta Ghebremedhin's (labor costs) diploma thesis.

ORCID iDs

Marta Ghebremedhin https://orcid.org/0000-0001-9225-2587
Christine Schreiber https://orcid.org/0000-0002-9825-0643
Thomas A Vilgis https://orcid.org/0000-0003-2101-7410

References

[1] Saha D and Bhattacharya S 2010 Hydrocolloids as thickening and gelling agents in food: a critical review *J. Food Sci. Technol.* **47** 587–97
[2] Chinachoti P 1995 Carbohydrates: functionality in foods *Am. J. Clin. Nutr.* **61** 922S–9S
[3] Phillips G O and Williams P A 2009 *Handbook of Hydrocolloids* (Amsterdam: Elsevier)
[4] Whistler R L and BeMiller J N 1993 *Industrial Gums: Polysacchraides and Their Derivates. Industrial Gums* 3rd edn (Amsterdam: Elsevier)
[5] De Gennes P-G and Gennes P-G 1979 *Scaling Concepts in Polymer Physics* (Ithaca, NY: Cornell University Press)
[6] Zielbauer B I, Schönmehl N, Chatti N and Vilgis T A 2017 Networks: from rubbers to food *Adv. Polym. Sci.* **275** 187–233
[7] Tako M and Nakamura S 1989 Evidence for intramolecular associations in xanthan molecules in aqueous media *Agric. Biol. Chem.* **53** 1941
[8] Talashek T, Seheult M, Carter T, Navarrete R and Chang H 2003 Non-pyruvylated xanthan in oil field applications utilizing high density calcium-based brines *US Patent WO/2001/088058*
[9] Sworn G 2009 Xanthan Gum *Food Stabilisers, Thickeners and Gelling Agents* ed A Imeson (Oxford: Wiley-Blackwell) pp 325–42
[10] Nordqvist D and Vilgis T A 2011 Rheological study of the gelation process of agarose-based solutions *Food Biophys.* **6** 450–60
[11] Dea I C M and Morris E R 1977 Synergistic xanthan gels *Extracellular Microb. Polysaccharides* **13** 174–82
[12] Moorhouse R, Walkinshaw M D and Arnott S 1977 Xanthan gum - molecular conformation and interactions *Extracellular Microb. Polysaccharides* **7** 90–102
[13] Morris E R, Rees D A, Young G, Walkinshaw M D and Darke A 1977 Order-disorder transition for a bacterial polysaccharide in solution. A role for polysaccharide conformation in recognition between Xanthomonas pathogen and its plant host *J. Mol. Biol.* **110** 1–16
[14] Kawamura Y 2008 Carob bean gum chemical and technical assessment (CTA) *69th JECFA* **1** 1–6
[15] Kawamura Y 2008 GUAR GUM Chemical and Technical Assessment *Pas Un Vrai Artic.* **1** 2–5
[16] Mudgil D, Barak S and Khatkar B S 2014 Guar gum: processing, properties and food applications - a review *J. Food Sci. Technol.* **51** 409–18
[17] Barak S and Mudgil D 2014 Locust bean gum: processing, properties and food applications—a review *Int. J. Biol. Macromol.* **66** 74–80

[18] Goycoolea F M, Milas M and Rinaudo M 2001 Associative phenomena in galactomannan-deacetylated xanthan systems *Int. J. Biol. Macromol.* **29** 181–92
[19] Parry J-M 2009 Konjac Glucomannan *Food Stabilisers, Thickeners and Gelling Agents*, ed A Imeson (Oxford: Wiley-Blackwell) pp 199–215
[20] Li L, Ruan H, Ma -L-L, Wang W, Zhou P and He G-Q 2009 Study on swelling model and thermodynamic structure of native konjac glucomannan *J. Zhejiang Univ. Sci.* B **10** 273–9
[21] Wang C, Zhang Y, Huang H, Chen M and Li D 2011 Solution conformation of konjac glucomannan single helix *New Adv. Mater. Pts 1 2* **197–198** 96–104
[22] Dea I C M, Morris E R, Rees D A, Welsh E J, Barnes H A and Price J 1977 Associations of like and unlike polysaccharides: mechanism and specificity in galactomannans, interacting bacterial polysaccharides, and related systems *Carbohydr. Res.* **57** 249–72
[23] Cairns P, Miles M J and Morris V J 1986 Intermolecular binding of xanthan gum and carob gum *Nature* **322** 89–90
[24] Shatwell K P, Sutherland I W, Ross-Murphy S B and Dea I C M 1990 Influence of the acetyl substituent on the interaction of xanthan with plant polysaccharides—I. Xanthan-locust bean gum systems *Carbohydr. Polym.* **14** 29–51
[25] Shatwell K P, Sutherland I W, Ross-Murphy S B and Dea I C M 1990 Influence of the acetyl substituent on the interaction of xanthan with plant polysaccharides—II. Xanthan-guar gum systems *Carbohydr. Polym.* **14** 115–30
[26] Shatwell K P, Sutherland I W, Ross-Murphy S B and Dea I C M 1990 Influence of the acetyl substituent on the interaction of xanthan with plant polysaccharides—III. Xanthan-konjac mannan systems *Carbohydr. Polym.* **14** 131–47
[27] Tako M 1991 Synergistic interaction between deacylated xanthan and galactomannan *J. Carbohydr. Chem.* **10** 619–33
[28] Tako M 1993 Binding sites for mannose-specific interaction between xanthan and galactomannan, and glucomannan *Colloids Surf.* B **1** 125–31
[29] Tako M, Teruya T, Tamaki Y and Ohkawa K 2010 Co-gelation mechanism of xanthan and galactomannan *Colloid Polym. Sci.* **288** 1161–6
[30] Abbaszadeh A, Macnaughtan W, Sworn G and Foster T J 2016 New insights into xanthan synergistic interactions with konjac glucomannan: A novel interaction mechanism proposal *Carbohydr. Polym.* **144** 168–77
[31] Copetti G, Grassi M, Lapasin R and Pricl S 1997 Synergistic gelation of xanthan gum with locust bean gum: A rheological investigation *Glycoconj. J.* **14** 951–61
[32] Brownsey G J and Morris V J 1987 Mixed and filled gels: models for foods *Food Struct. Its Interact. evalution, Eds* pp 7–23
[33] Cairns P, Miles M J, Morris V J and Brownsey G J 1987 X-ray fibre-diffraction studies of synergistic, binary polysaccharide gels *Carbohydr. Res.* **160** 411–23
[34] Cheetham N W H and Mashimba E N M 1990 Conformational aspects of xanthan—Galactomannan gelation. Further evidence from optical-rotation studies *Carbohydr. Polym.* **14** 17–27
[35] Cheetham N W H and Mashimba E N M 1988 Conformational aspects of xanthan-galactomannan gelation *Carbohydr. Polym.* **9** 195–212
[36] Dea I C M, Clark A H and McCleary B V 1986 Effect of galactose-substitution-patterns on the interaction properties of galactomannas *Carbohydr. Res.* **147** 275–94
[37] Davé V and McCarthy S 1997 Review of konjac glucomannan *J. Polym. Environ.* **5** 237–41
[38] Williams P A, Day D H, Langdon M J, Phillips G O and Nishinari K 1991 Synergistic interaction of xanthan gum with glucomannans and galactomannans *Food Hydrocoll.* **4** 489–93
[39] Wehr R 2017 Korrelation der Primärstruktur von Xanthanen mit deren Verhalten in Lösung, Johannes Gutenberg-Universität Mainz, Germany
[40] Mezger T G 2010 *Das Rheologie Handbuch: Für Anwender von Rotations- und Oszillations-Rheometern* (Hannover: Vincentz Network)
[41] Vilgis T A 2012 Hydrocolloids between soft matter and taste: culinary polymer physics *Int. J. Gastron. Food Sci.* **1** 46–53
[42] Winter H H 1987 Can the gel point of a cross-linking polymer be detected by the G′ – G″ crossover? *Polym. Eng. Sci.* **27** 1698–702
[43] Williams P A *et al* 2004 New forms of xanthan gum with enhanced properties *Gums and Stabilisers for the Food Industry 12* eds P A Williams and G O Phillips (Cambridge: The Royal Society of Chemistry) pp 124–30
[44] Morris V J 2006 Bacterial Polysaccharides *Food Polysaccharides and Their Applications*, ed A M Stephen, G O Phillips and P Williams (Boca Raton, FL: CRC Press) pp 413–54
[45] Tako M and Nakamura S 1984 Rheological properties of deacetylated xanthan in aqueous media *Agric. Biol. Chem.* **48** 2987–93
[46] Annable P, Williams P A and Nishinari K 1994 Interaction in xanthan-glucomannan mixtures and the influence of electrolyte *Macromolecules* **27** 4204–11